Thickness matters
in self-gravitating expanding shells

R. Wünsch J. E. Dale J. Palouš S. Ehlerová V. Sidorin
A. P. Whitworth R. Smith S. Walch J. Dawson Y. Fukui

Based on:

Dale, J. E., Wünsch, R., Whitworth, A., Palouš, J., 2009, MNRAS, 398, 1537
Wünsch, R., Dale, J. E., Palouš, J., Whitworth, A., 2010, MNRAS, 407, 1963
Dale, J. E., Wünsch, R., Smith, R. J. et al., 2010, MNRAS, 411,2230
Wünsch, R., Jáchym, P., Sidorin, V., et al., 2011, A&A, submitted

Outline:

1. **Observations of shells**
   → shells are everywhere
2. **Pressure Assisted Gravitational Instability**
   → AMR vs. SPH simulations vs. theory
   → Derivation of PAG and the mass spectrum
3. **APEX observations of the Carina Flare supershell**
   → Observational test of PAGI

Galactic bubble N107, Credit: Churchwell et al. (2006), Spitzer, GLIMPSE, IRAC, 8μm cont.

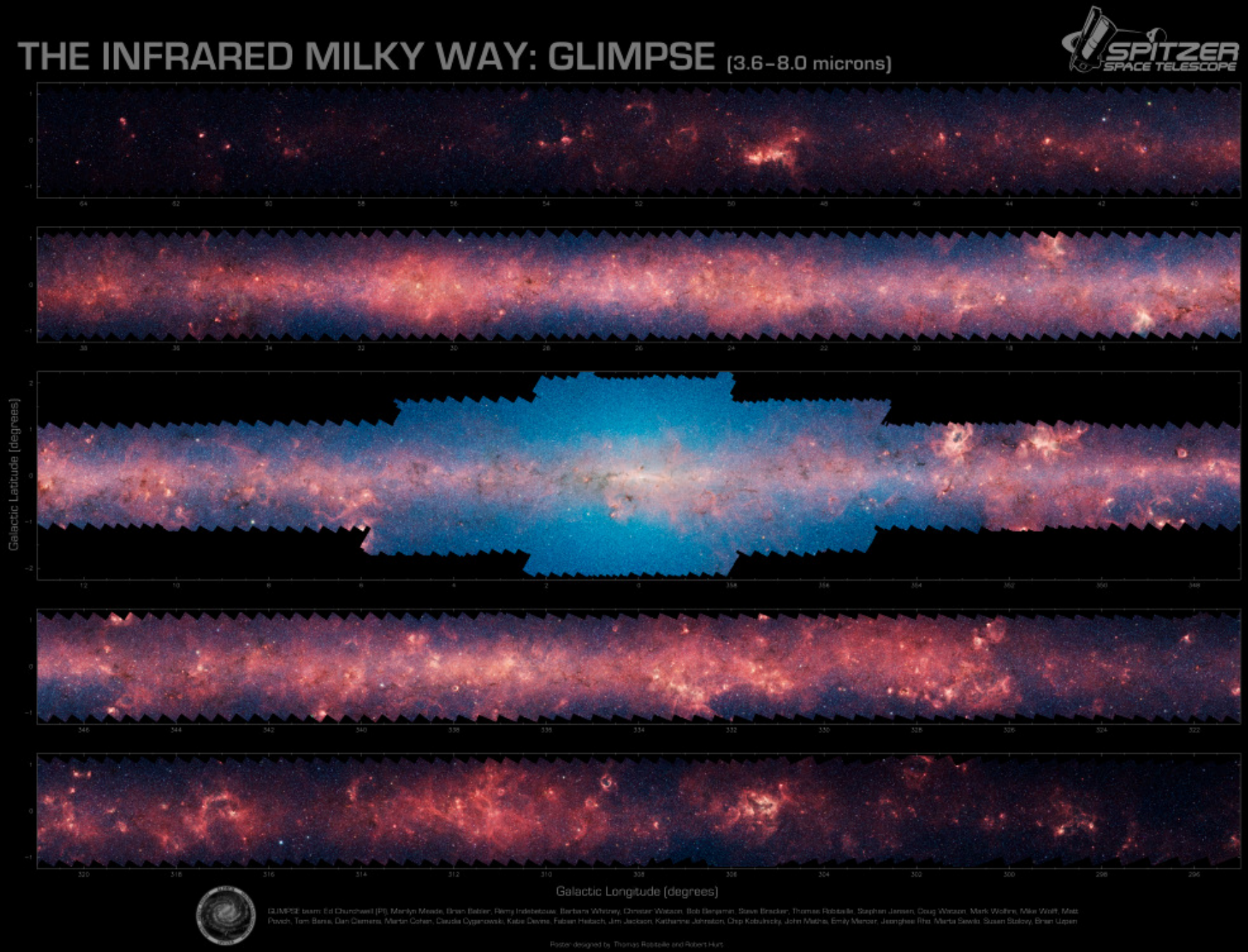
THE INFRARED MILKY WAY: GLIMPSE (3.6–8.0 microns)
SPITZER SPACE TELESCOPE
Galactic Latitude (degrees)
Galactic Longitude (degrees)
GLIMPSE team: Ed Churchwell (PI), Marilyn Meade, Brian Babler, Remy Indebetouw, Barbara Whitney, Christer Watson, Bob Benjamin, Steve Bracker, Thomas Robitaille, Stephen Jansen, Doug Watson, Mark Wolfire, Mike Wolff, Matt Povich, Tom Bania, Dan Clemens, Martin Cohen, Claudia Cyganowski, Kate Devine, Fabian Heitsch, Jim Jackson, Katherine Johnston, Chip Kobulnicky, John Mathis, Emily Mercer, Jeonghee Rho, Marta Sewilo, Susan Stolovy, Brian Uzpen
Poster designed by Thomas Robitaille and Robert Hurt

The bubbling galactic disk

(Churchwell et al., 2006)

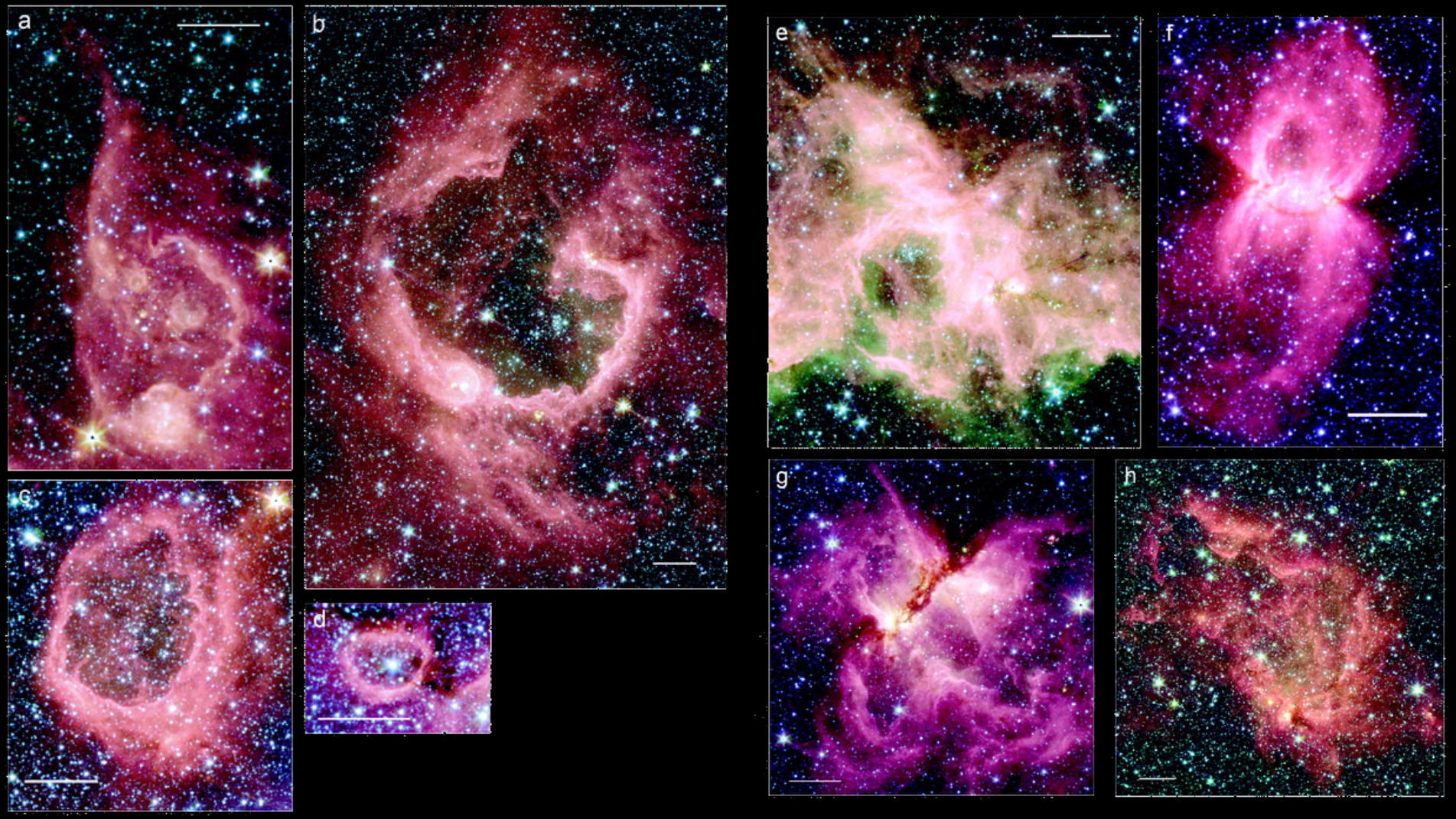

Spitzer bands: 4.5μm (blue), 5.8μm (green), 8μm (red)

Bubbles are everywhere

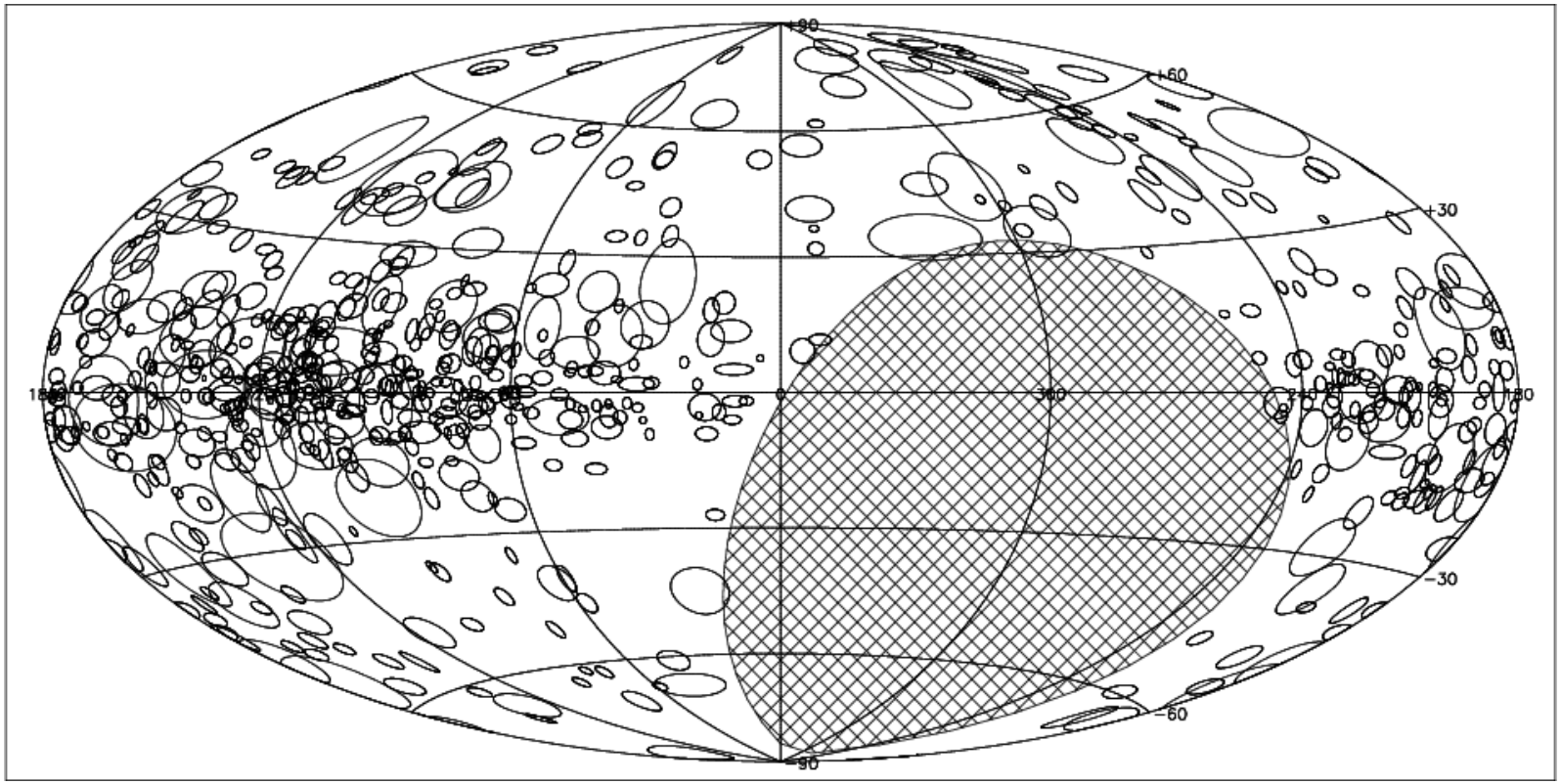

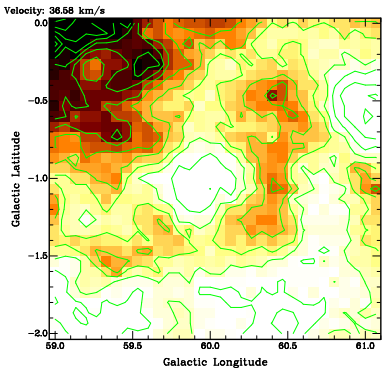

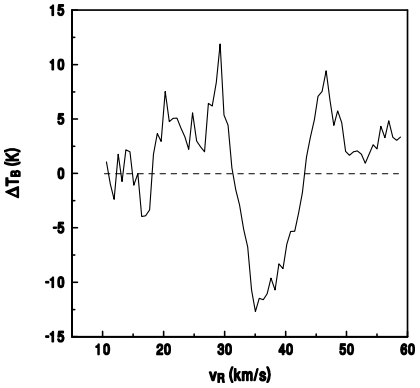

automatic search for HI shells in Leiden-Dwingeloo survey
→ statistical study of 300 HI shells in 2nd quadrant
(Ehlerová et al. 2005)

Bubble properties

- radii: $r \sim 10$ pc - 2 kpc
- expansion velocities: $v_{\rm exp} \sim 5 - 30$ km/s
- formation energy: $E \sim 10^{51} - 10^{53}$ erg
- observed in many wavelengths: HI (IGALFA, . . .), IR (Spitzer/GLIMPSE,. . .), Hα (WHAM), mm (CO lines), radio cont., X-rays
- observed in MW and many nearby galaxies (LMC, SMC, M31, M33, IC10 . . .)
- origin: OB stars (fossils of expanding HII regions), encounters with HVC or dwarf galaxy, GRB, turbulence and instabilities in ISM
- implications: source of information about ISM, Disk-halo connection, **Triggered star formation (Collect and Collapse)**

Collect and collapse

(Elmegreen & Lada, 1977)

HII region Sh 104 (Deharveng et al., 2003)

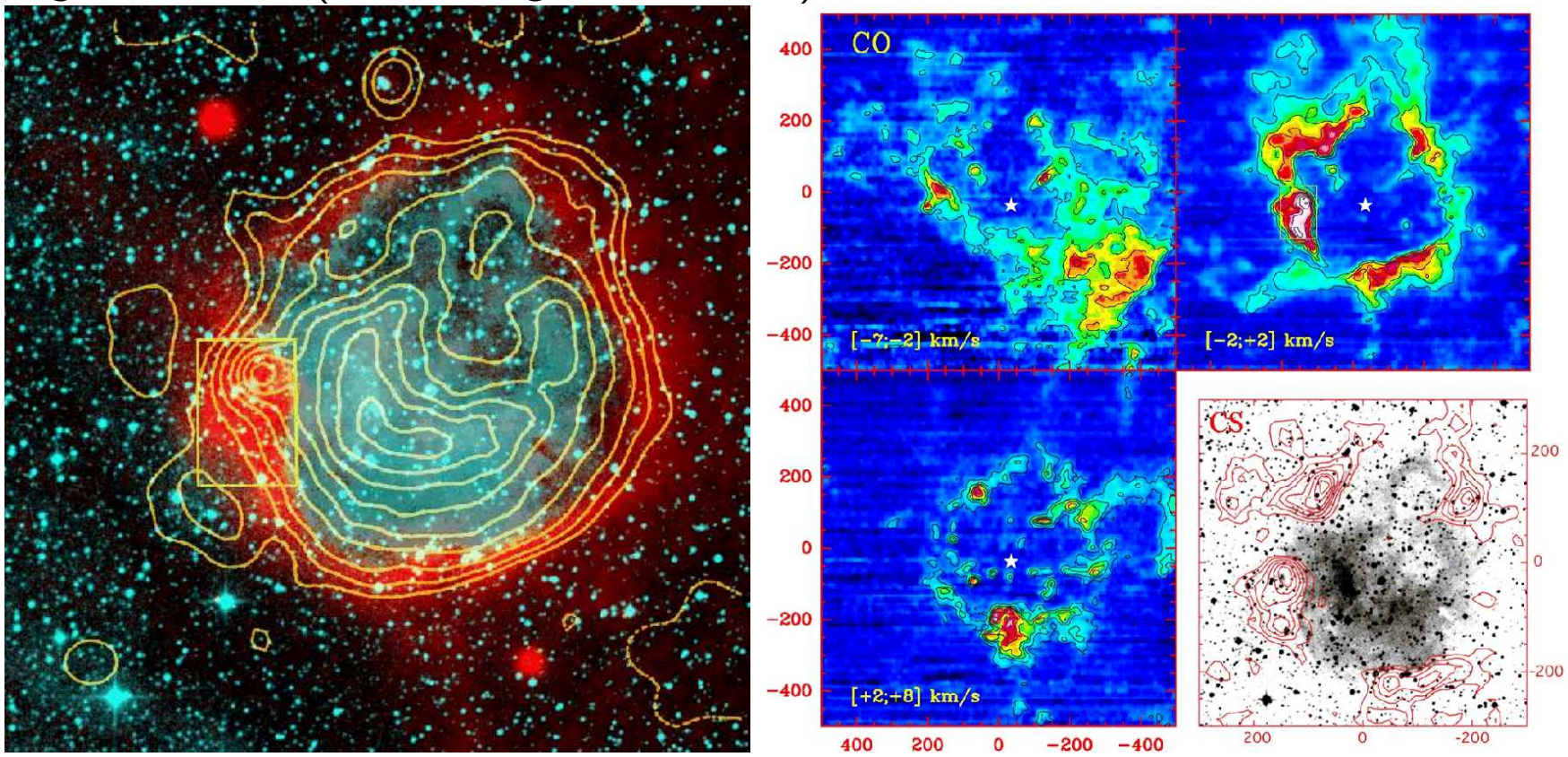

Left: contours (thermal radio continuum 1.46 GHz), red (mid-IR emmision - PAHs), turquoise (Hα - ionized gas)
Right: CO molecular line at different velocities

Multiwavelength study of N107

(Sidorin, 2008)

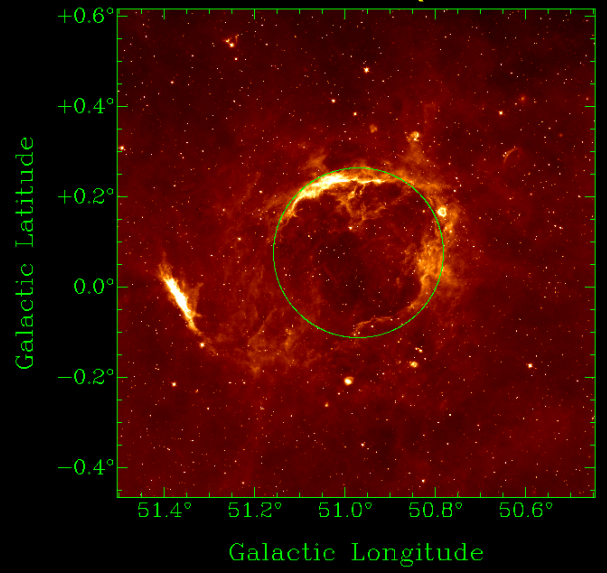

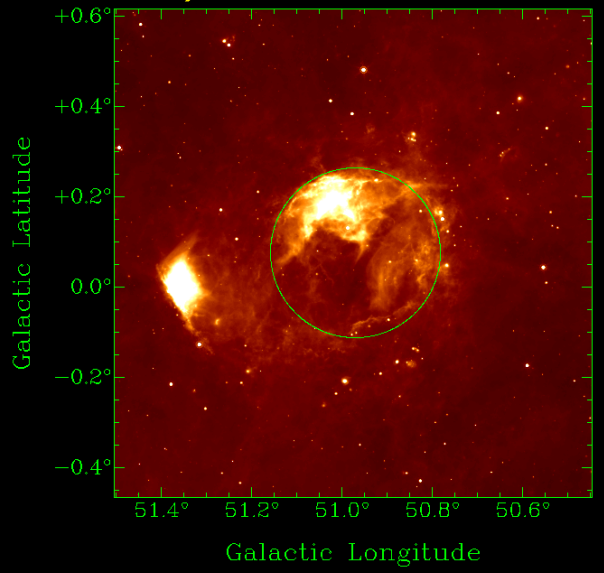

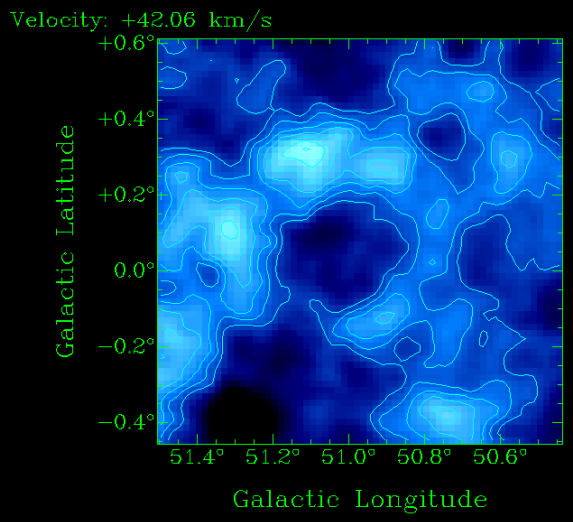

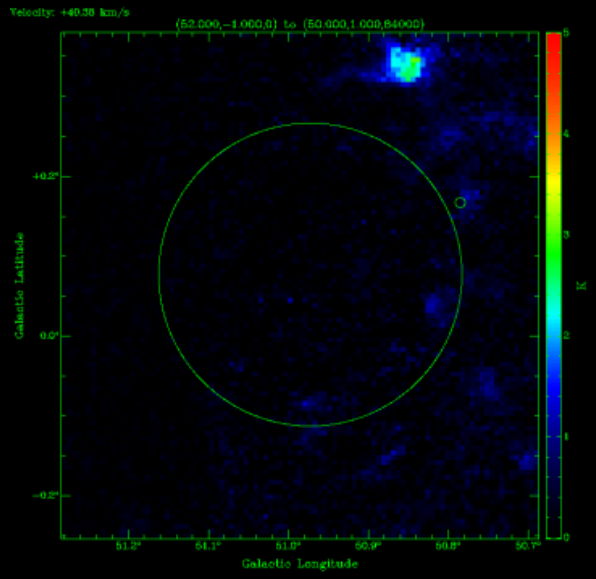

Expanding shell instabilities

- gravitational instability (long time-scale)
- Rayleigh-Taylor instability

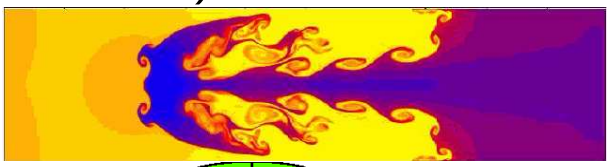

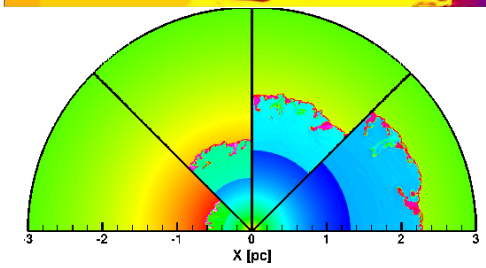

- Vishniac instability
  (Vishniac, 1983; 1994)
- magnetic field:
  Parker inst. (Parker 1966)

  Wardle inst. (Wardle, 1990)

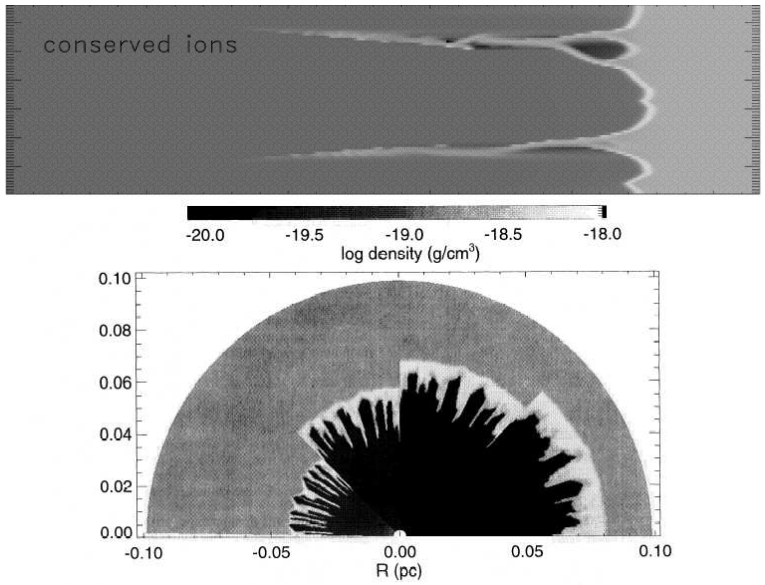

FIG. 6.—Evolution of the I-S front instability for a case with constant density (model UC32). The cooling cutoff is 10^3 K, and the time step is 5×10^3 yr. The ambient medium has $n_0 = 10^3$ cm^{-3} and $T_0 = 100$ K, and the stellar flux is $F_* = 10^{48}$ s^{-1}. This model is equivalent to the very early stages of model S32, shown in Fig. 8.

- ionized shell instability
  (Garcia-Segura & Franco, 1996)

Simulation setup

- extremely simplified model to avoid instabilities other than the gravitational one
  (RT, Vishniac)
- ballistic shell (in a free fall) embedded in a rarefied medium

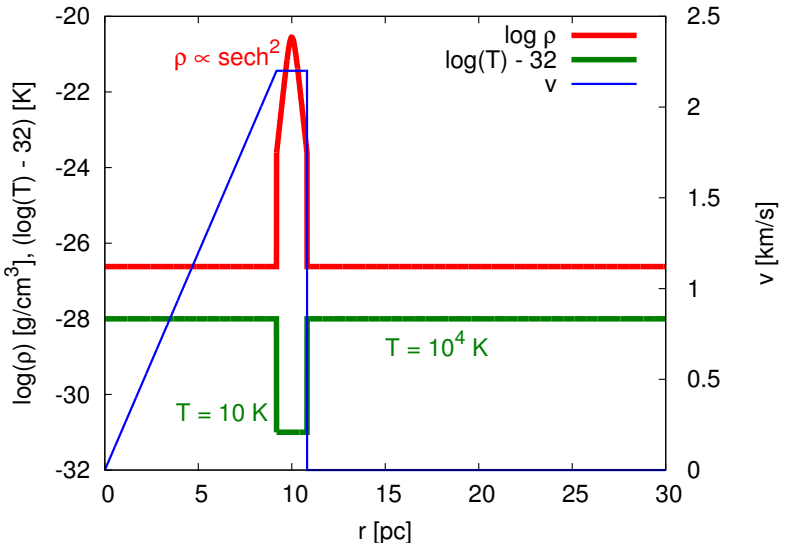

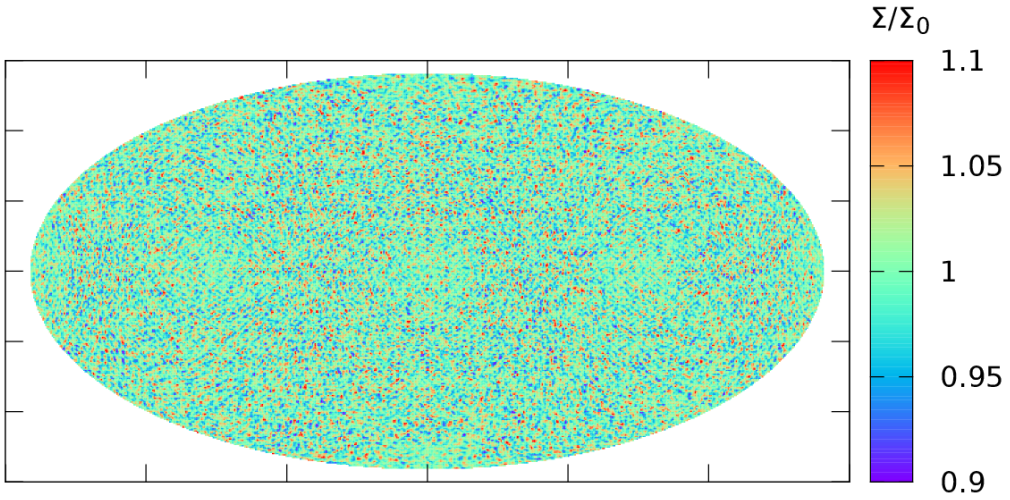

$M_{\rm shell} = 2 \times 10^4$ M$_\odot$
$T_{\rm shell} = 10$ K
$R_{\rm shell,0} = 10$ pc
$V_{\rm shell,0} = 2.2$ km s^{-1}
$R_{\rm shell,max} = 23$ pc
$P_{\rm ext} = 10^{-17}$, 10^{-13}
or 5×10^{-13} dyne cm^{-2}

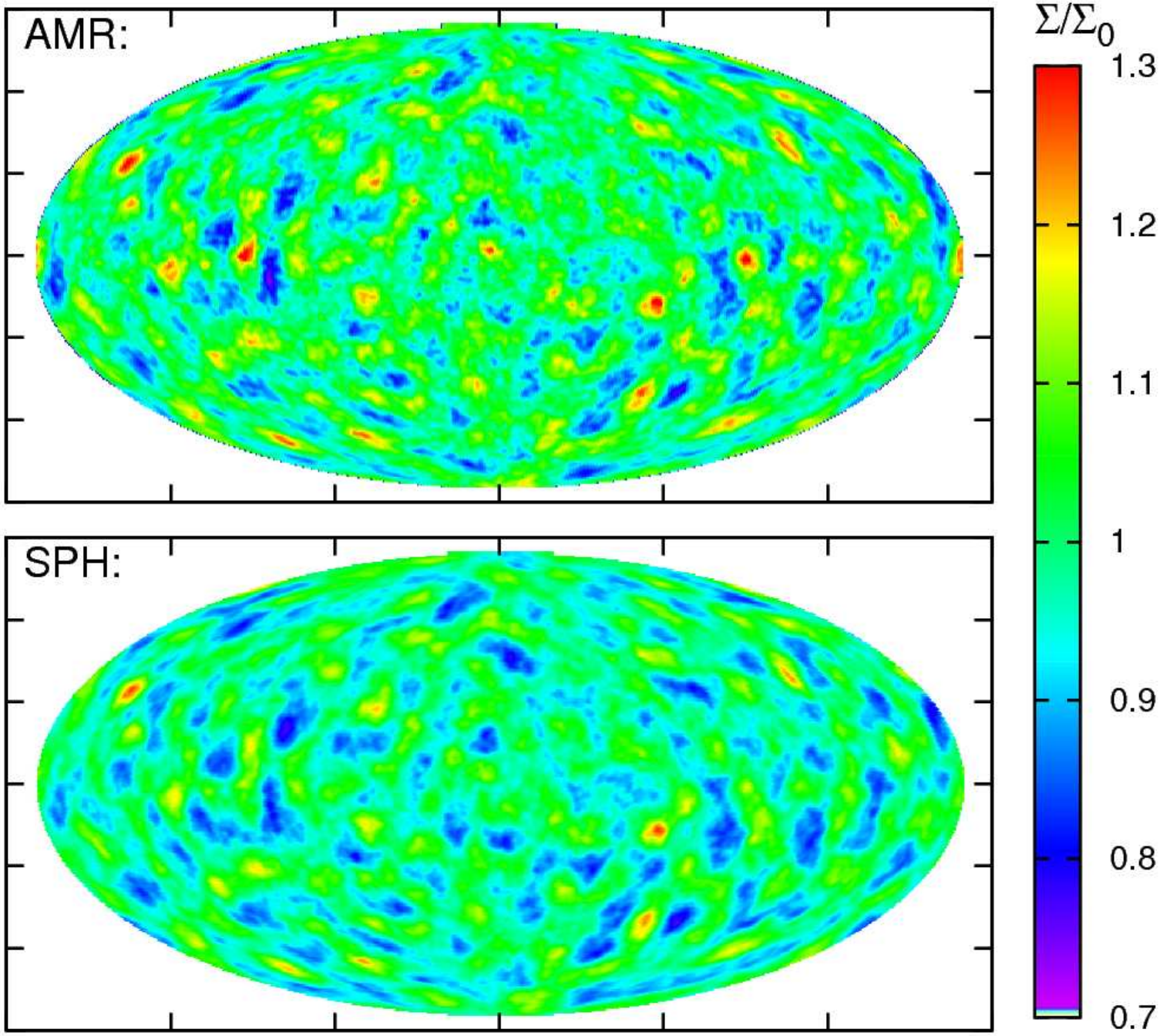
AMR:
SPH:
Σ/Σ_0
1.3
1.2
1.1
1
0.9
0.8
0.7

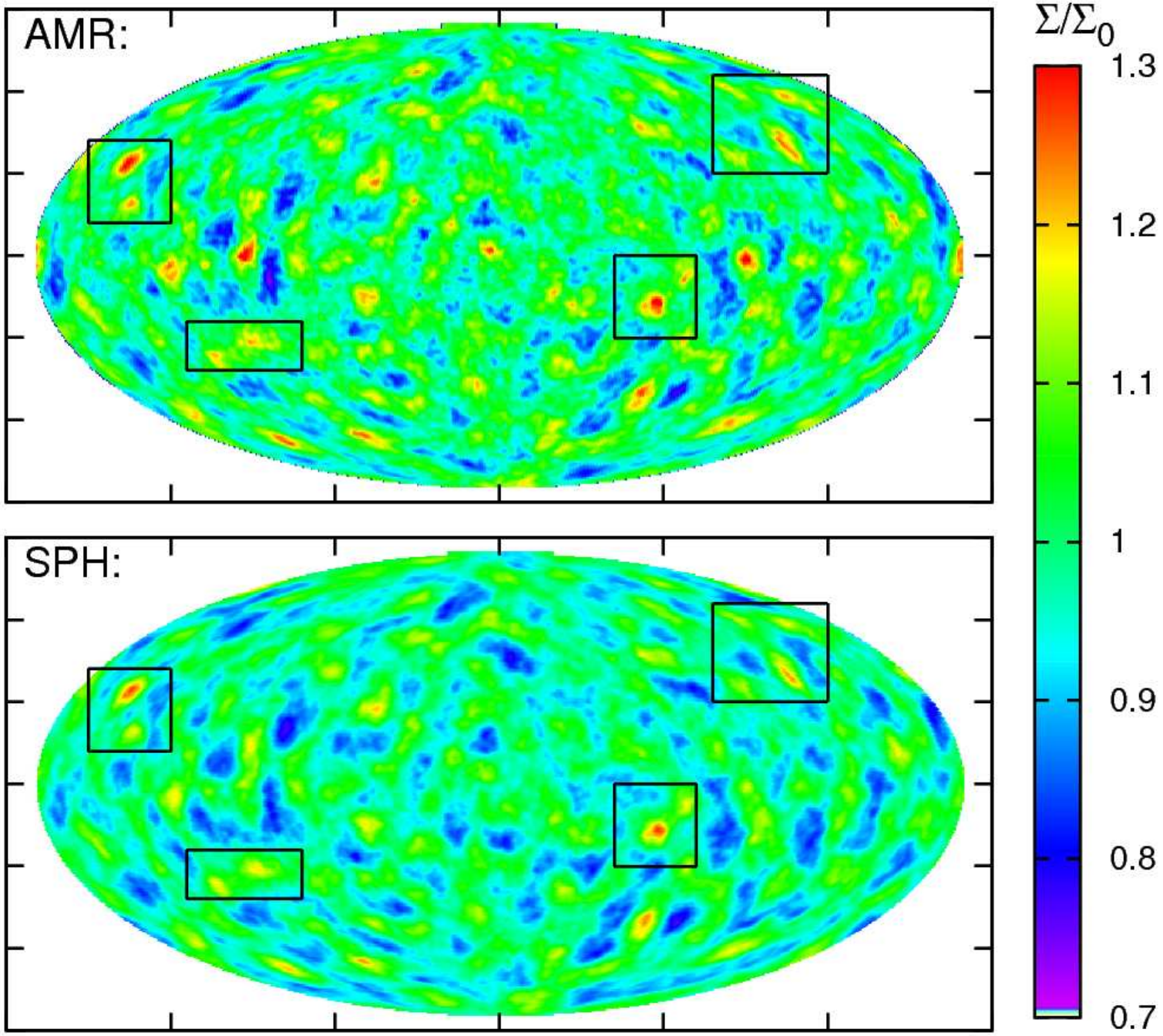
AMR:
SPH:
Σ/Σ_0
1.3
1.2
1.1
1
0.9
0.8
0.7

Find six differences!

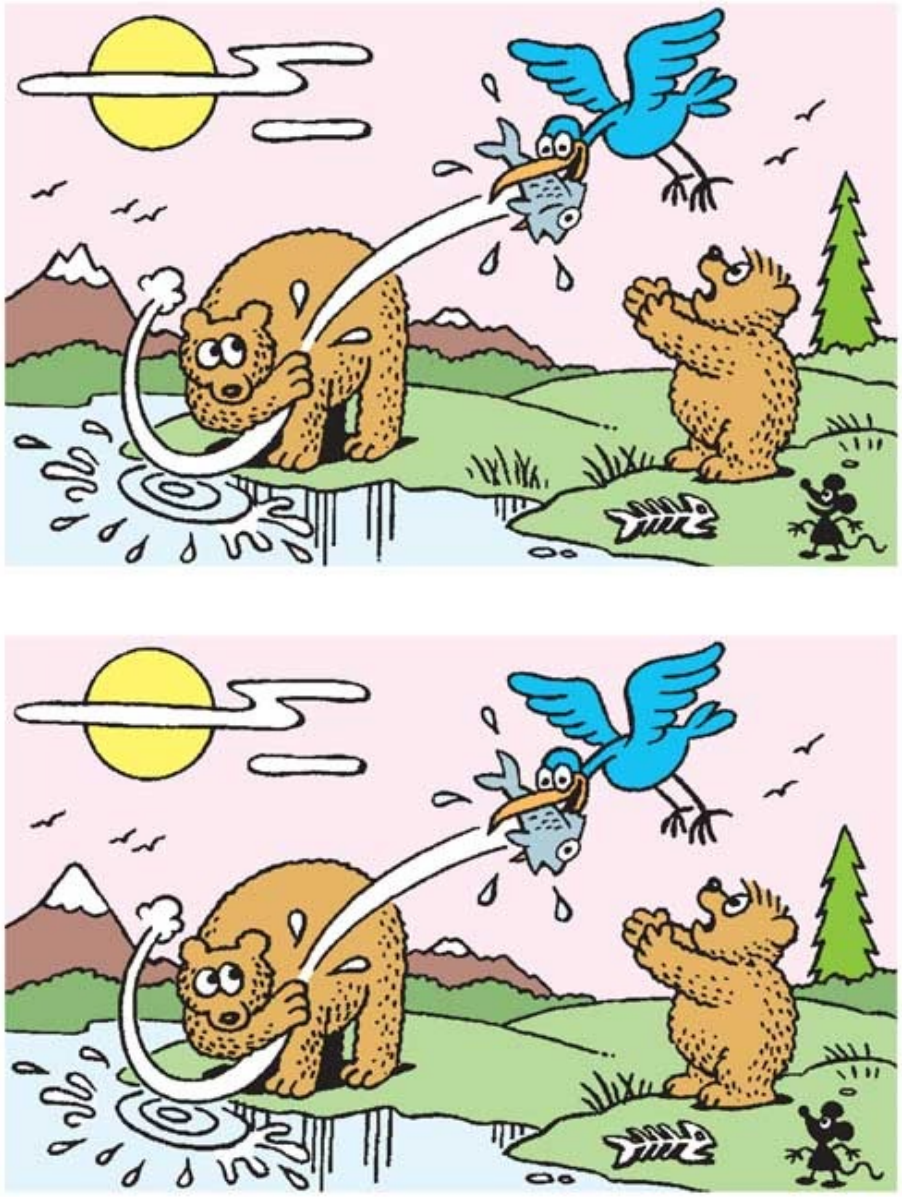

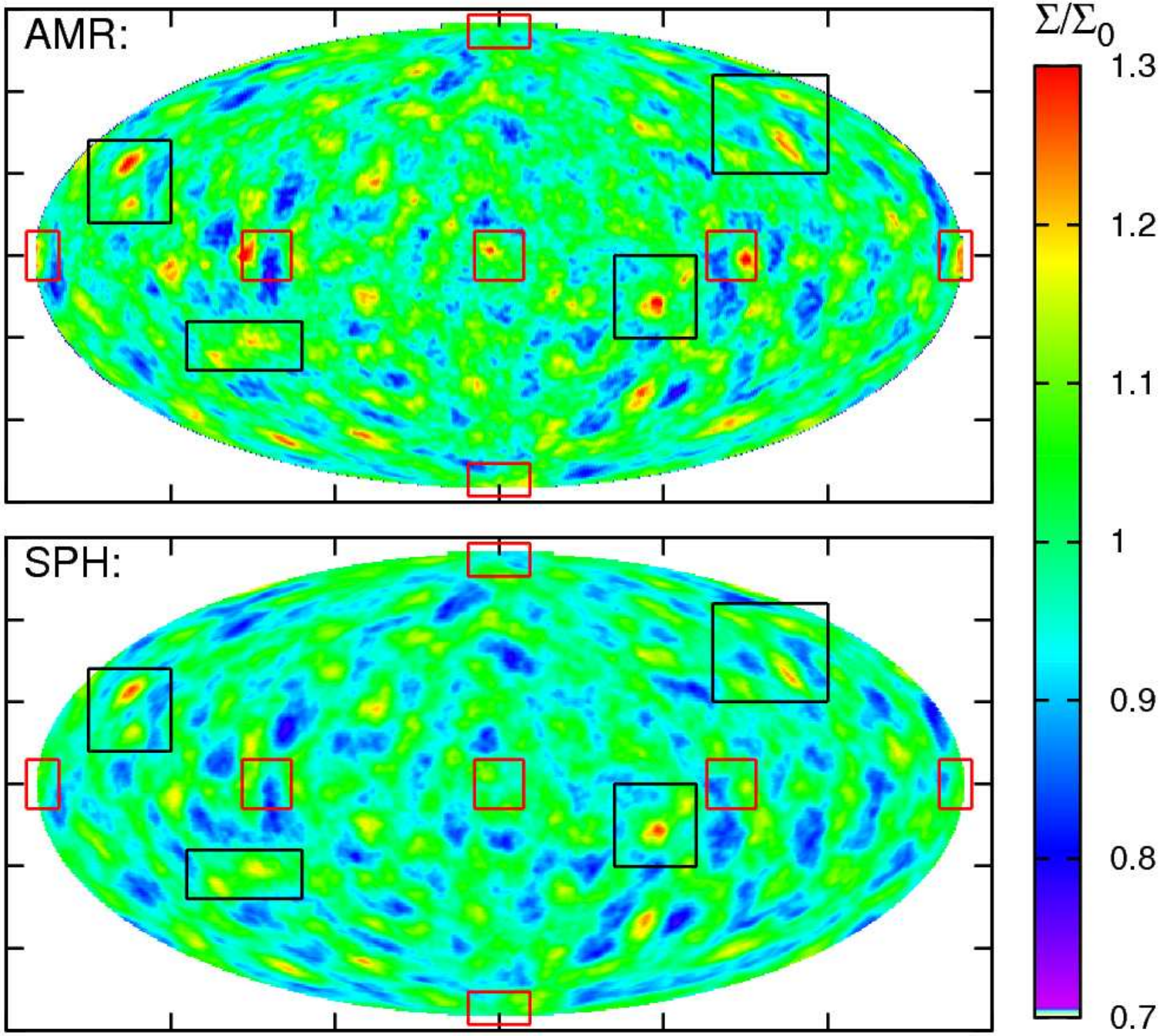
AMR:
SPH:
Σ/Σ_0
1.3
1.2
1.1
1
0.9
0.8
0.7

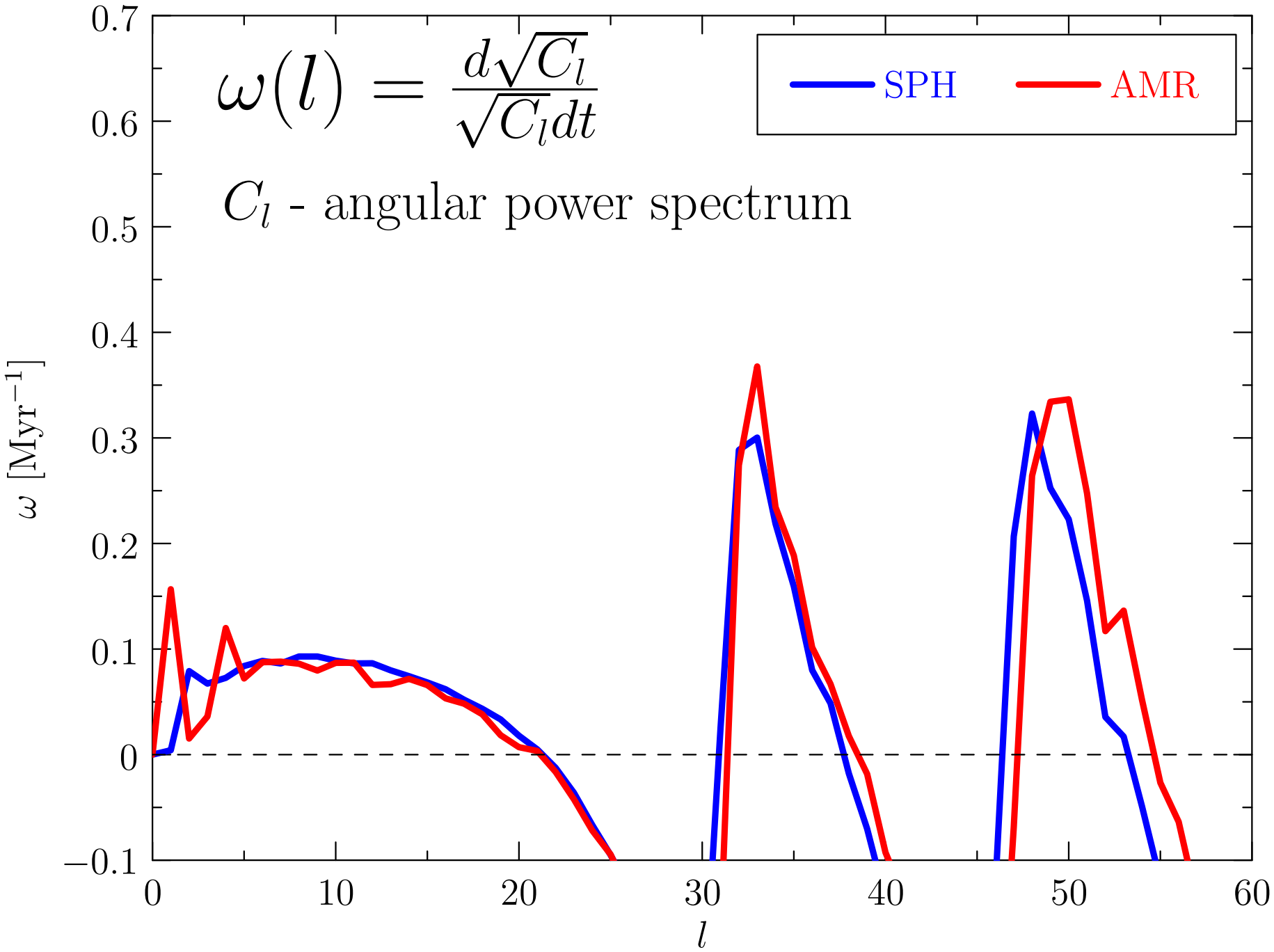
$\omega(l) = \frac{d\sqrt{C_l}}{\sqrt{C_l}dt}$
C_l - angular power spectrum
SPH
AMR
ω [Myr^{-1}]
l
0.7
0.6
0.5
0.4
0.3
0.2
0.1
0
−0.1
0
10
20
30
40
50
60

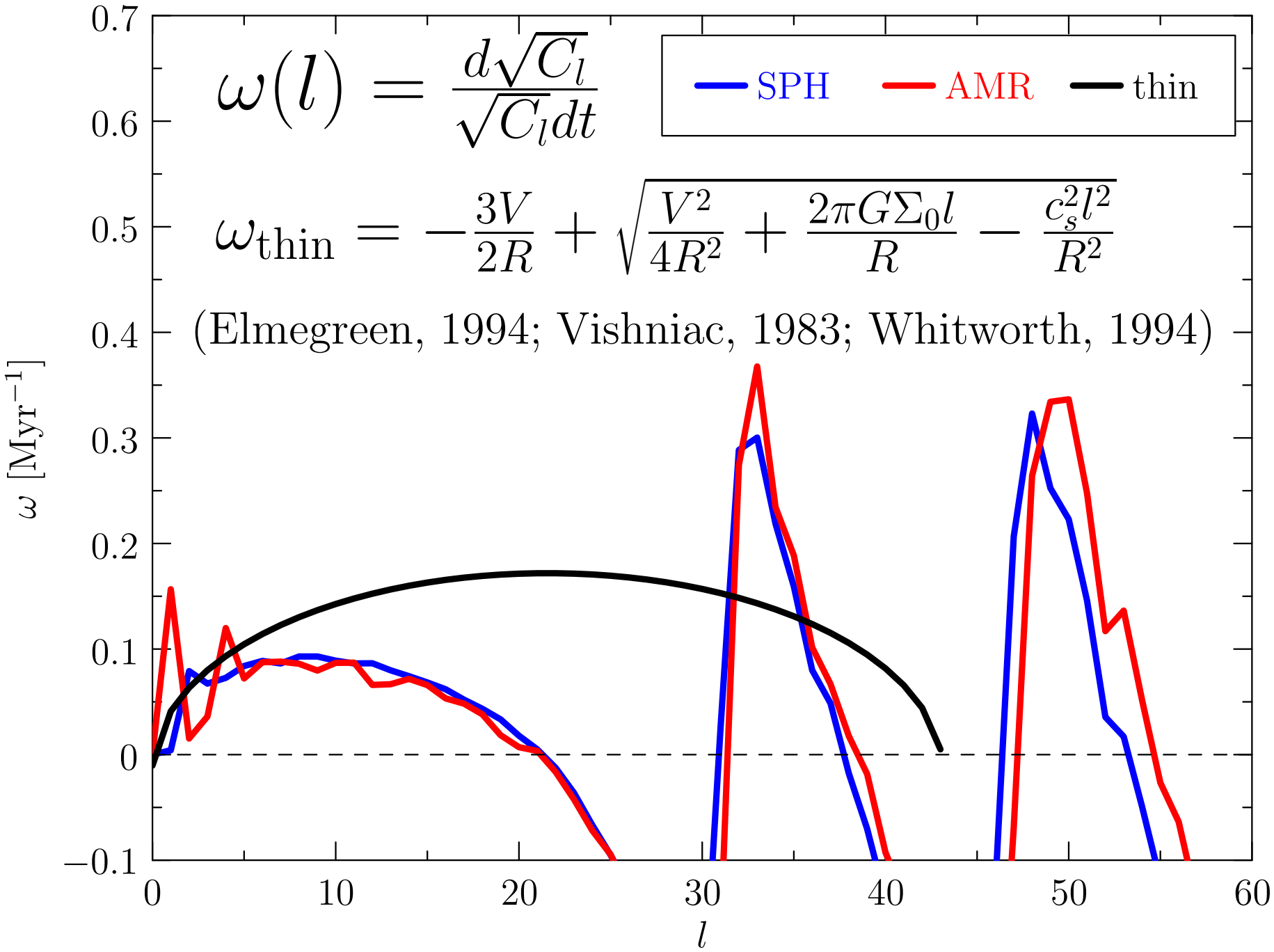
$\omega(l) = \frac{d\sqrt{C_l}}{\sqrt{C_l}dt}$
SPH
AMR
thin
$\omega_{\rm thin} = -\frac{3V}{2R} + \sqrt{\frac{V^2}{4R^2} + \frac{2\pi G\Sigma_0 l}{R} - \frac{c_s^2 l^2}{R^2}}$
(Elmegreen, 1994; Vishniac, 1983; Whitworth, 1994)
ω [Myr^{-1}]
l
0.7
0.6
0.5
0.4
0.3
0.2
0.1
0
−0.1
0
10
20
30
40
50
60

Gravitational instability of thin shell

(Vishniac, 1983; Whitworh et al. 1994; Elmegreen, 1994)

pressure gravity stretching accretion

$$\Sigma_0 R\frac{\partial \mathbf{\Omega}}{\partial t} = -c_s^2\nabla\Sigma_1 + \Sigma_0\nabla\Phi_1 - \Sigma_0\mathbf{\Omega}V - 3\Sigma_0\mathbf{\Omega}V$$

$$\frac{\partial\Sigma_1}{\partial t} = -\Sigma_0 R\nabla_{\mathrm{T}}\cdot\mathbf{\Omega} - 2\Sigma_1\frac{V}{R}$$

stretching

$$\nabla^2\Phi_1 = 4\pi G\Sigma_1\delta(r-R)$$

linearized perturbed equations, perturbations: $\Sigma = \Sigma_0 + \Sigma_1$, $\mathbf{\Omega}$, $\Phi = \Phi_0 + \Phi_1$

Fourier modes: $\Sigma_1 = \sum_{\mathbf{k}} \Sigma_{\mathbf{k}} \exp(\mathbf{k}\cdot\mathbf{r})$, $\Omega = \sum_{\mathbf{k}} \Omega_{\mathbf{k}} \exp(\mathbf{k}\cdot\mathbf{r})$, $\Phi_1 = \sum_{\mathbf{k}} \Phi_{\mathbf{k}} \exp(\mathbf{k}\cdot\mathbf{r})$

solution: . . . $(\dot\Sigma_{\mathbf{k}}, \dot\Omega_{\mathbf{k}}, \dot\Phi_{\mathbf{k}}) \sim \exp[\omega_l(t)]$

eigenvalues: growth rate of a mode with dimensionless wavenumber $l = kR$:

$$\omega_{\mathrm{thin}}(l) = -\frac{3V}{R} + \sqrt{\frac{V^2}{R^2} + \frac{2\pi G\Sigma_0 l}{R} - \frac{c_s^2 l^2}{R^2}}$$

High pressure ambient medium

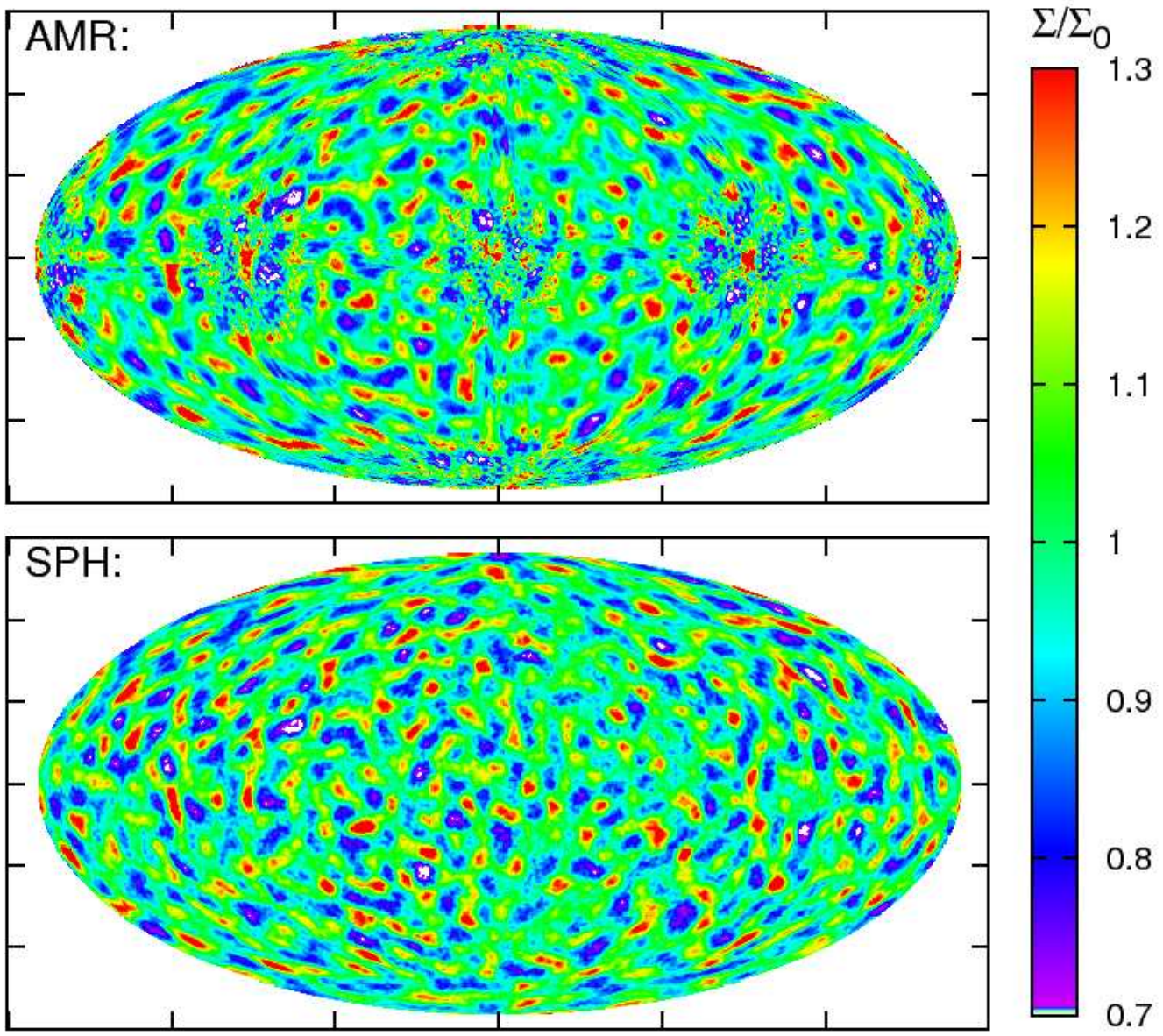

High pressure ambient medium

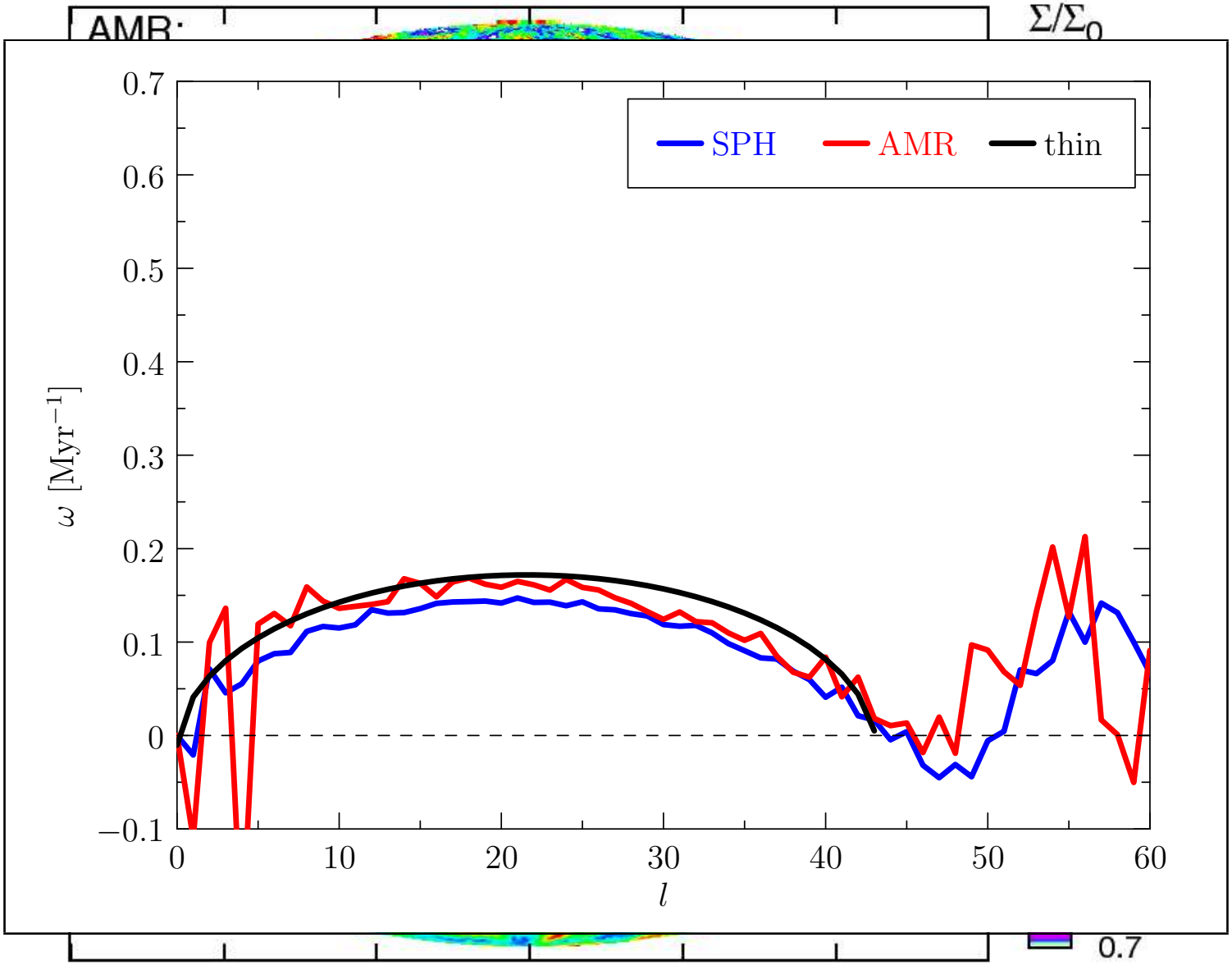

Dispersion relation depends on $P_{\rm ext}$ (and hence on the shell thickness)

$P_{\rm ext} = 10^{-17}$ $P_{\rm ext} = 10^{-13}$ $P_{\rm ext} = 5 \times 10^{-13}$dyne cm^{-2}

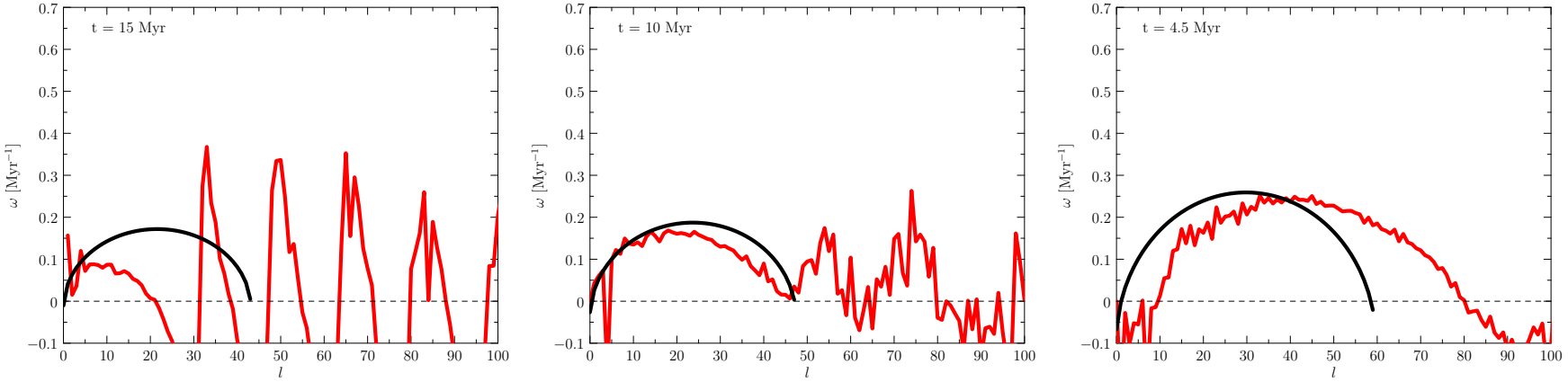

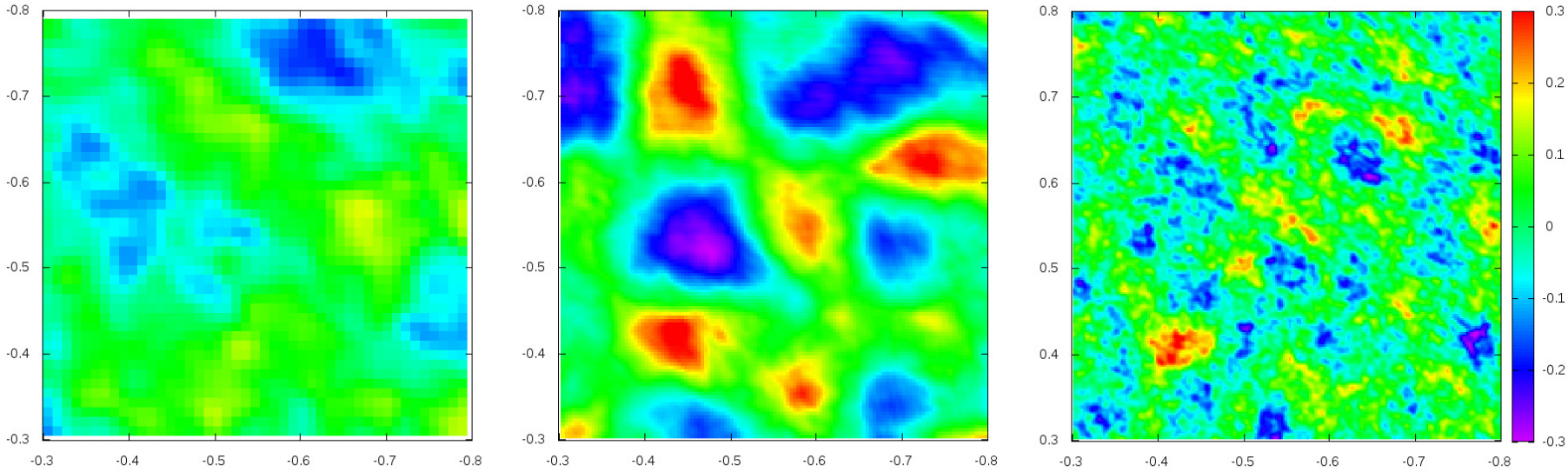

Dependence of fragment growth rate on $P_{\rm ext}$

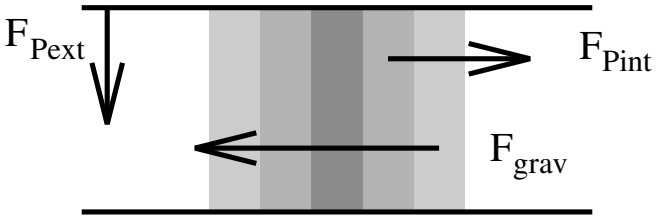

thin shell approx.

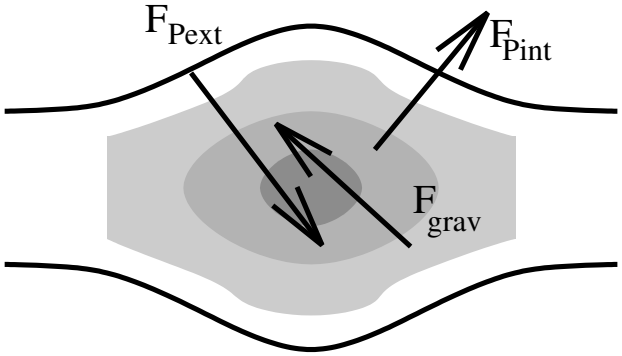

fragments in simulations

- the shell thickness varies across fragments
- external pres. force is not perpendicular to the shell surface

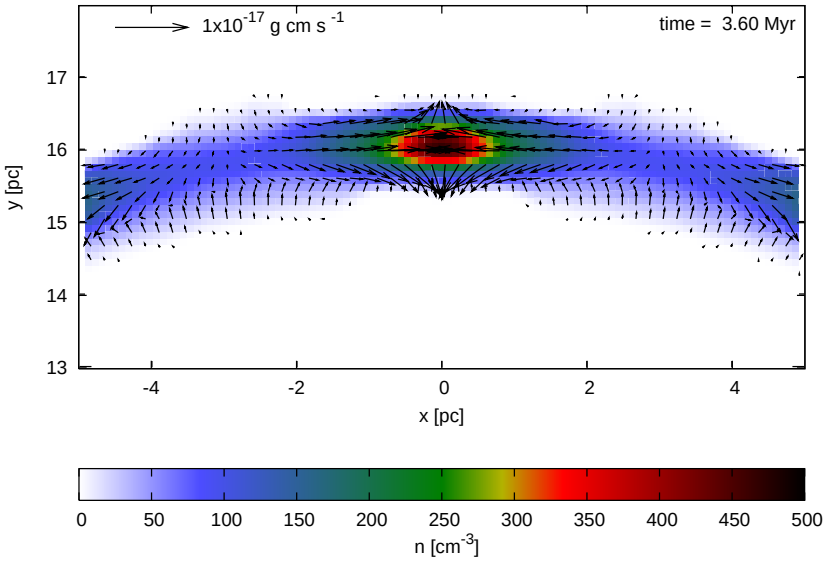

Uniform Oblate Spheroid

(Boyd & Whitworth, 2005)

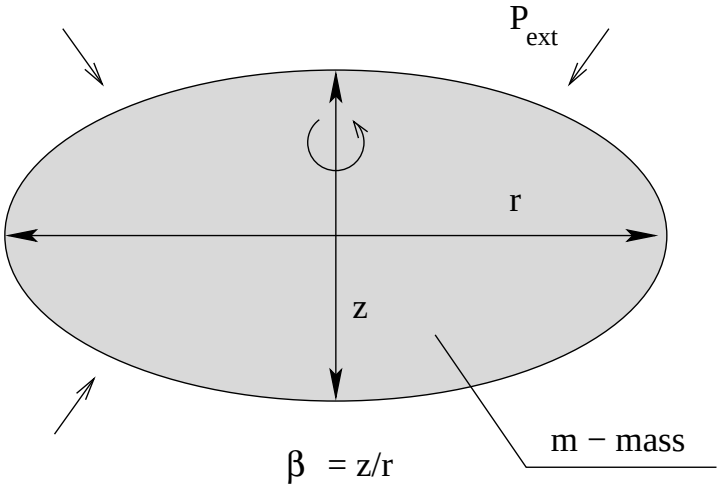

Kinetic, gravitational and compressional energy:

$$\mathcal{K} = \frac{m}{10}\left(2\dot{r}^2 + \dot{z}^2\right)$$

$$\mathcal{G} = -\frac{3\,G\,m^2}{5}\,\frac{\cos^{-1}(z/r)}{\left(r^2-z^2\right)^{1/2}}$$

$$\frac{d\mathcal{B}}{dV} = P_{\rm ext} - P_{\rm int} = P_{\rm ext} - \frac{m\,c_s^2}{V}$$

- energy conservation: $\mathcal{E} = \mathcal{K} + \mathcal{G} + \mathcal{B}$
- differentiate with resp. to time:

$$\left\{\frac{2\,m\,\ddot{r}}{5} + \frac{d\mathcal{G}}{dr} + \frac{d\mathcal{B}}{dr}\right\}\dot{r} + \left\{\frac{m\,\ddot{z}}{5} + \frac{d\mathcal{G}}{dz} + \frac{d\mathcal{B}}{dz}\right\}\dot{z} = 0\,.$$

- $\dot{r}$ and $\dot{z}$ independent:

$$\ddot{r} = -\frac{3Gm}{2r^2}\left[\frac{\cos^{-1}\beta}{(1-\beta^2)^{3/2}} - \frac{\beta}{1-\beta^2}\right] - \frac{20\pi P_{\rm ext} r z}{3m} + \frac{5c_s^2}{r}$$

UOS vs. thin shell

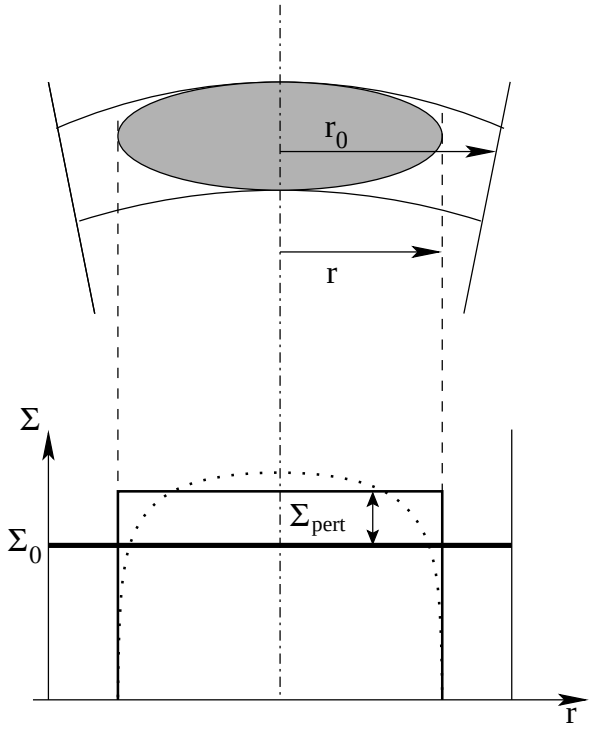

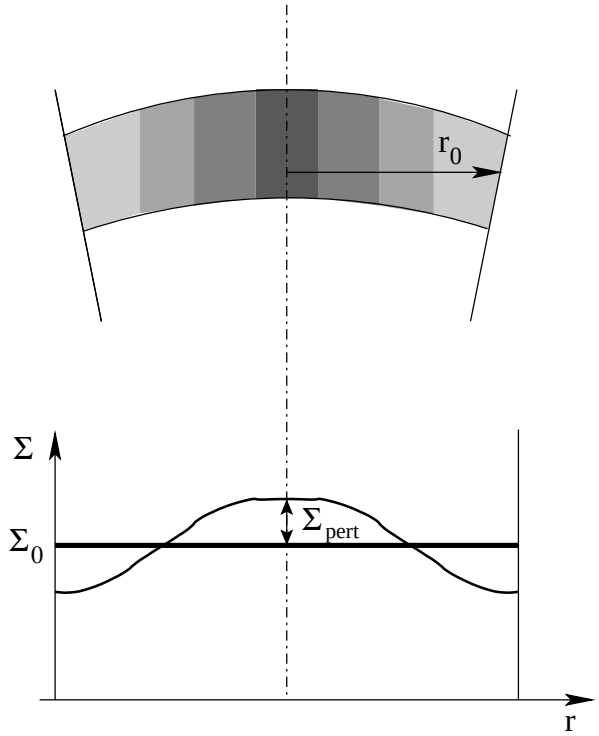

- z given by hydrostatic equilibrium
- non-linear eqs. of motion
- homogeneous ellipsoid

- no vertical structure (inf. thin shell)
- linearized hydrodyn. eqs.
- sinusoidal perturbations

Dispersion relation of the thick shell

$$\omega_\epsilon = -\underbrace{\frac{V}{2R\epsilon}}_{\text{stretching}} + \left\{ \underbrace{\frac{V^2}{4R^2\epsilon^2}}_{\text{stretching}} + \underbrace{\frac{3G\Sigma_0 l}{4R\epsilon}\left[\frac{\cos^{-1}\beta}{(1-\beta^2)^{3/2}} - \frac{\beta}{1-\beta^2}\right]}_{\text{gravity}} \right.$$

$$\left. + \underbrace{\frac{1 - P_{\text{ext}} c_s^2 l^2}{3\pi^2 R^2 \epsilon (2P_{\text{ext}} + \pi G \Sigma_0^2)}}_{\text{external pres.}} \underbrace{- \frac{5 c_s^2 l^2}{2\pi^2 R^2 \epsilon}}_{\text{internal pres.}} \right\}^{1/2} .$$

Conf. to thin shell:

$$\omega_{\text{thin}} = -\underbrace{\frac{3V}{2R}}_{\text{stretching}} + \left(\underbrace{\frac{V^2}{4R^2}}_{\text{stretching}} + \underbrace{\frac{2\pi G \Sigma_0 l}{R}}_{\text{gravity}} \underbrace{- \frac{c_s^2 l^2}{R^2}}_{\text{internal pres.}} \right)^{1/2}$$

- geometry factor at gravity term
- external pressure term
- dependence on ϵ - shrink fraction

Pressure assisted gravitational instability

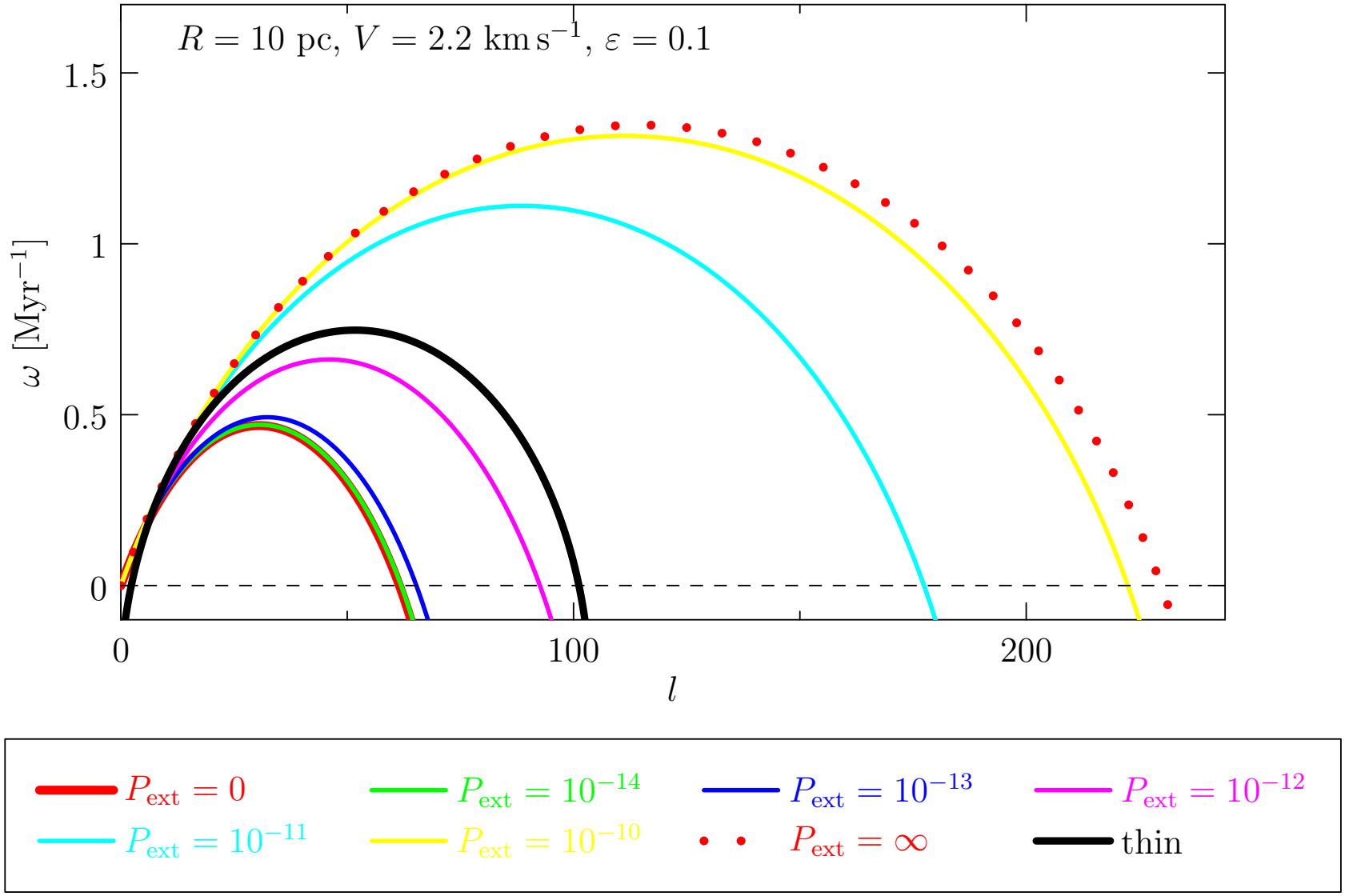

Critical external pressure: $\omega_\epsilon \sim \omega_{\rm thin}$

- $\omega_\epsilon \sim \omega_{\rm thin}$ for $P_{\rm ext,crit}$ for which $\frac{dz}{d\Sigma} = 0$
  (the shell thickness does not depend on the surface density)

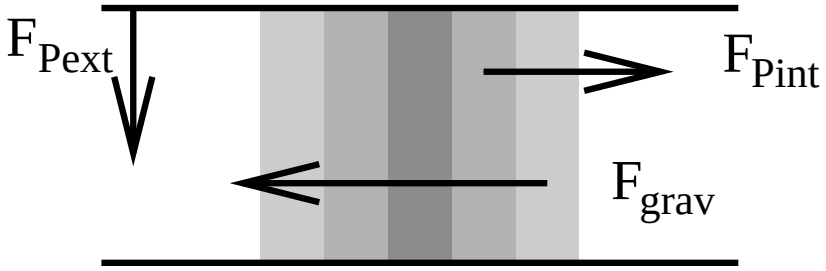

thin shell approx.

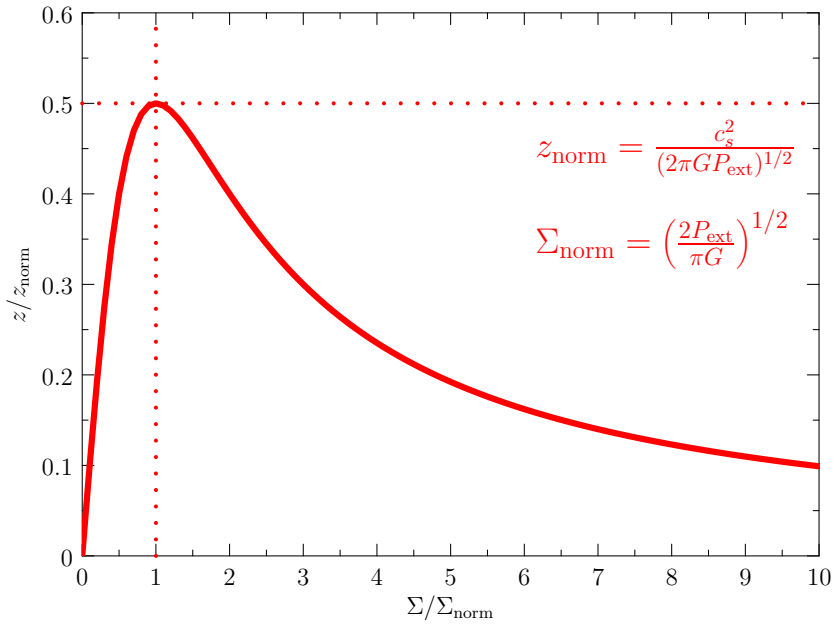

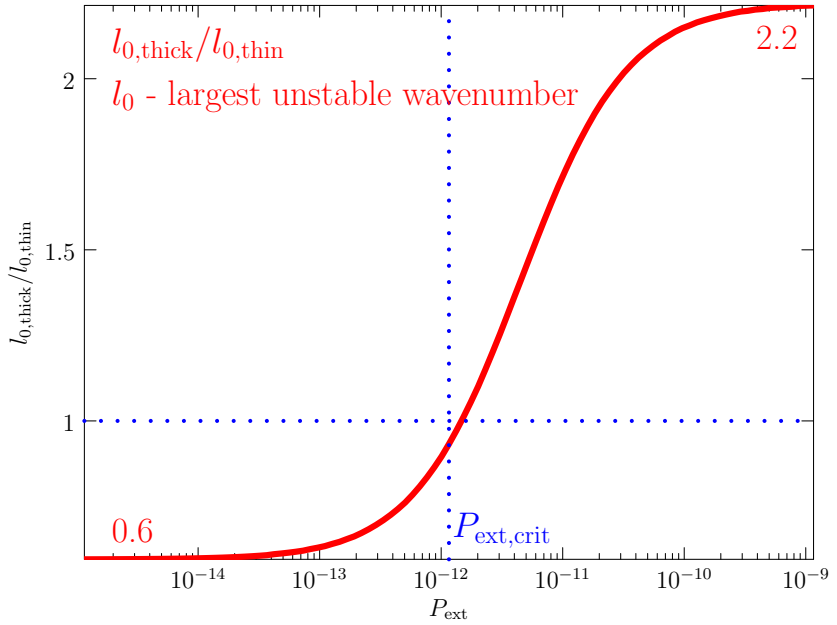

PAGI vs. simulations

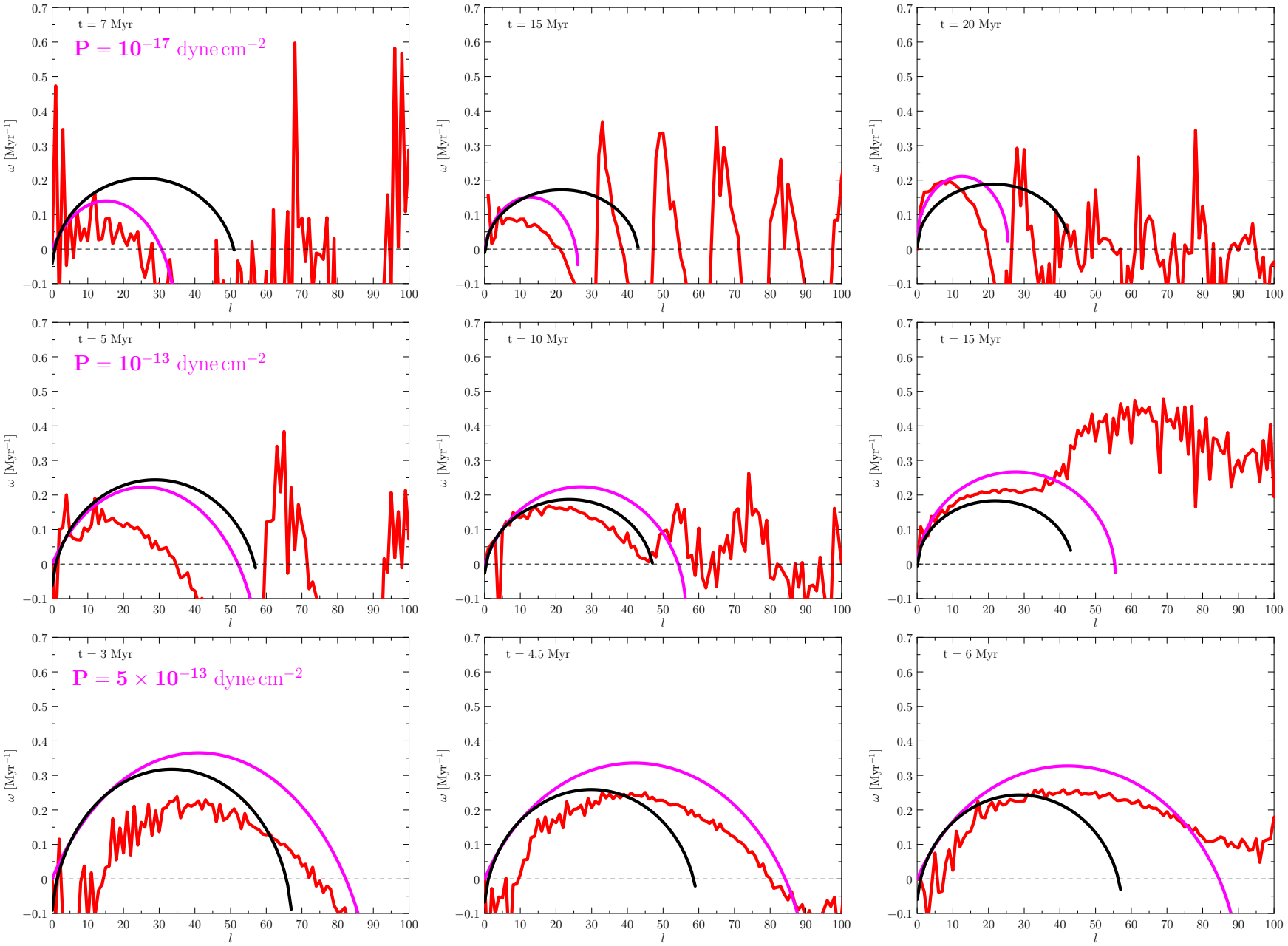

Mass spectrum from Fragmentation Integral

$$\frac{dN}{dm} \sim I_{\rm f}(l,t) \times m^{-2}$$

where $I_{\rm f}(l,t) = \int \omega(l,t')dt'$ is **the fragmentation integral**

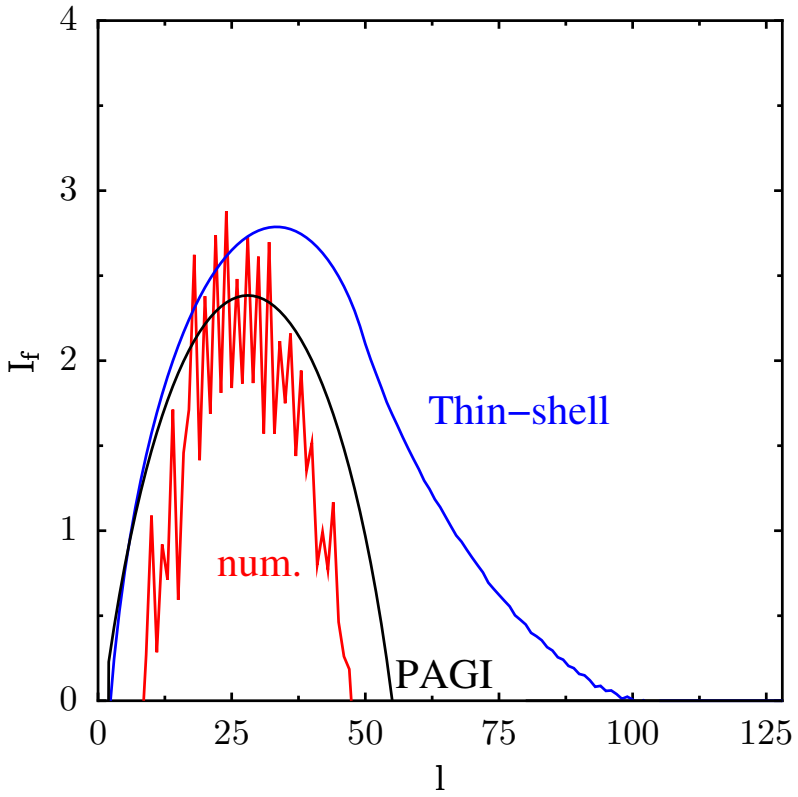

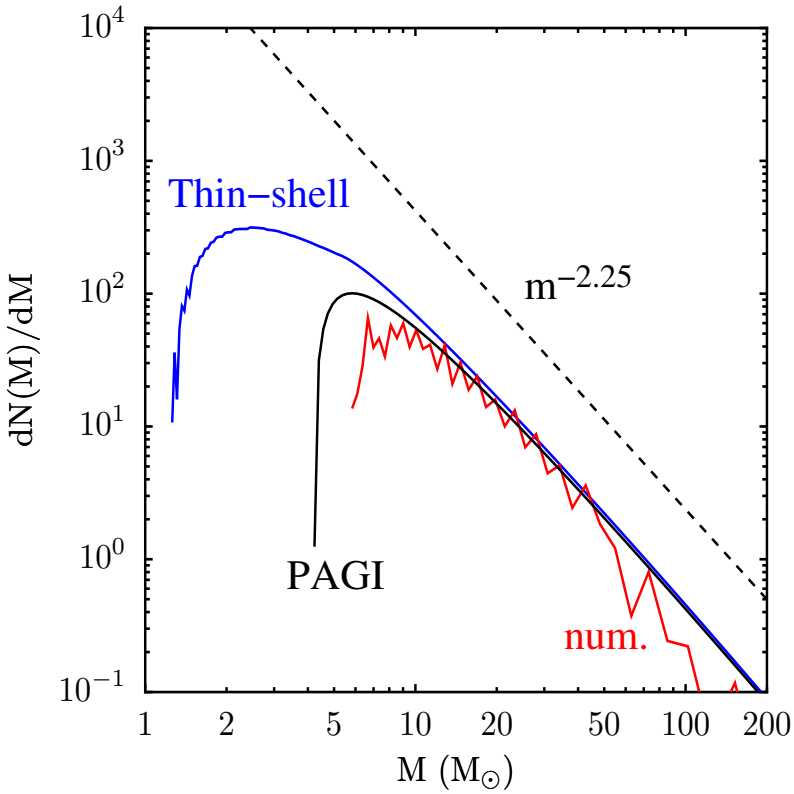

Mass spectrum of clumps

- clumps identified by algorithm by Smith et al (2009) (similar to CLUMPFIND, but uses grav. potential instead of density)
- initially agrees well with mass spectrum obtain from the fragmentation integral
- later, it becomes more and more top-heavy

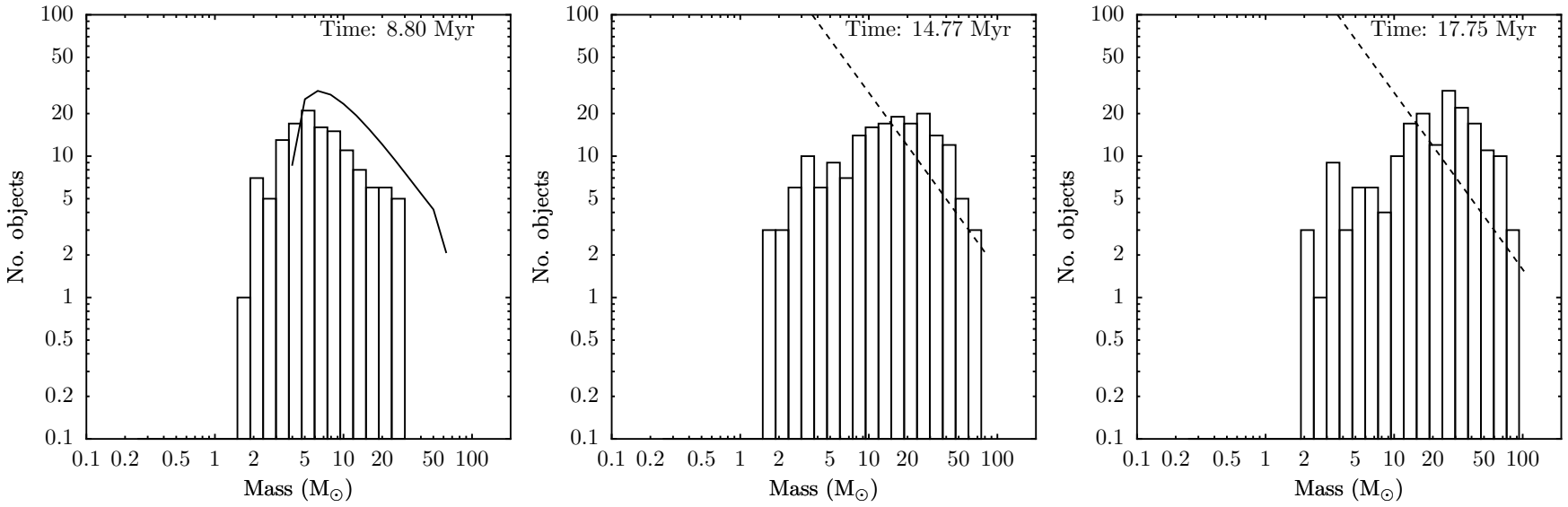

Carina Flare Supershell observarion

- we observe Carina Flare supershell with the APEX telescope (Atacama Pathfinder EXperiment)
- CF extends ~ 450 pc above the gal. pl. - different P_{EXT} expected
- two clouds (16 and 74) selected (based on NANTEN observations)
- Cloud 16 observed during ESO 86A period - 22 hours

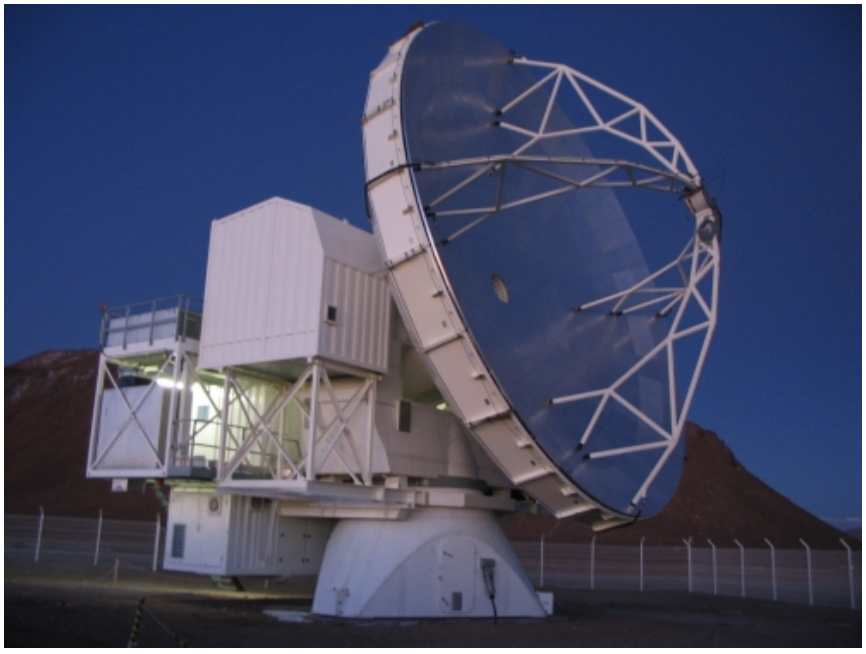

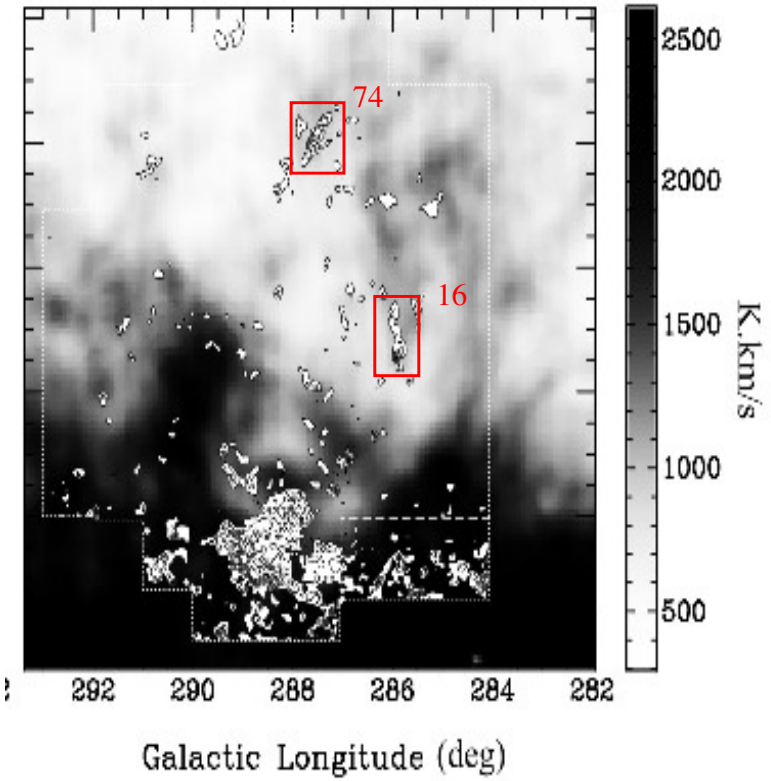

APEX and NANTEN obs. of Cloud 16

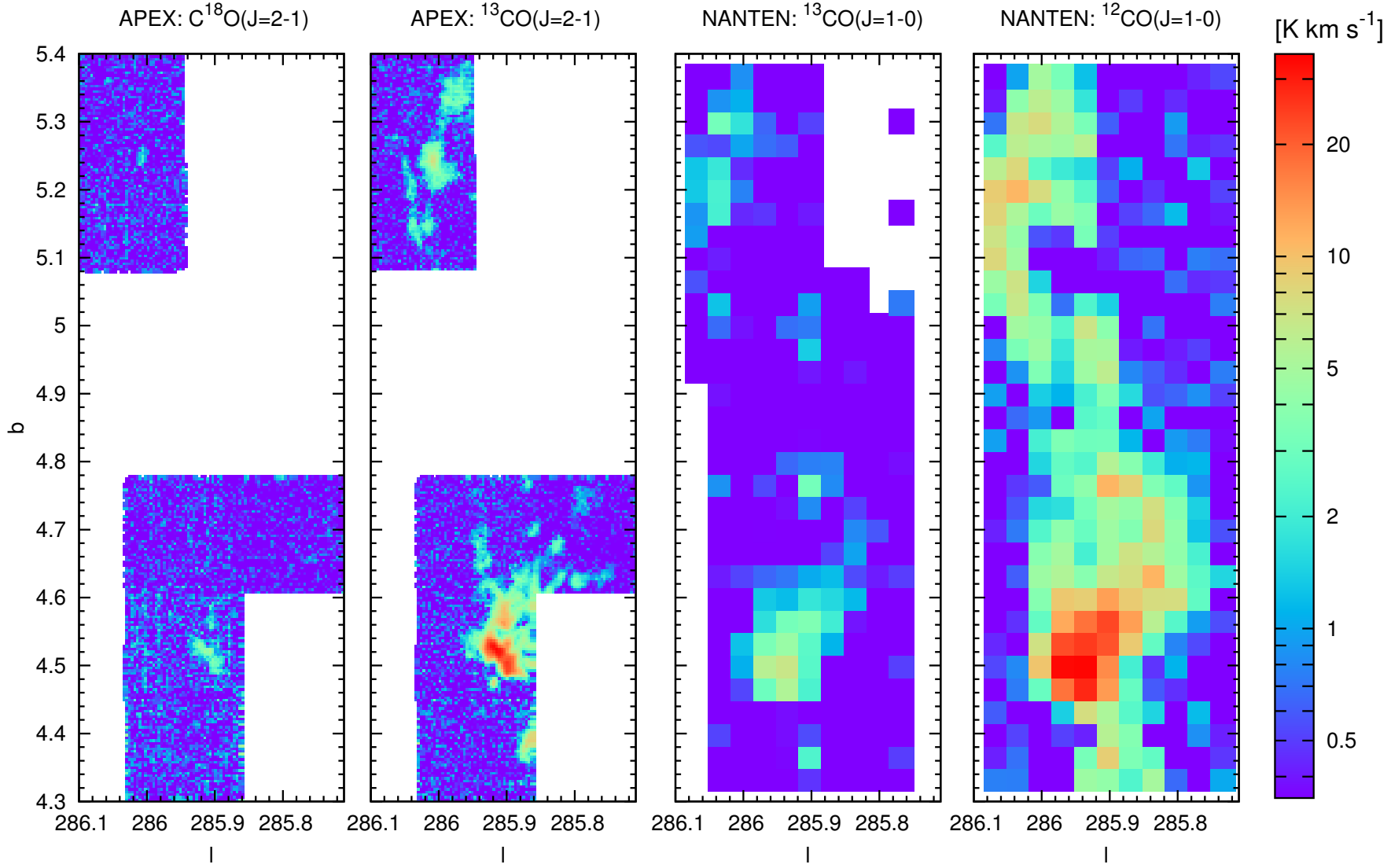

Identification of clumps

- clump-finding sw DENDROFIND (http://galaxy.asu.cas.cz/∼richard/dendrofind/)
- two essential parameters: `Tcutoff`, `dTleaf`

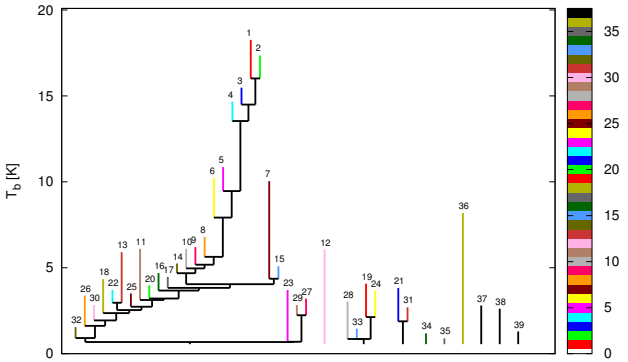

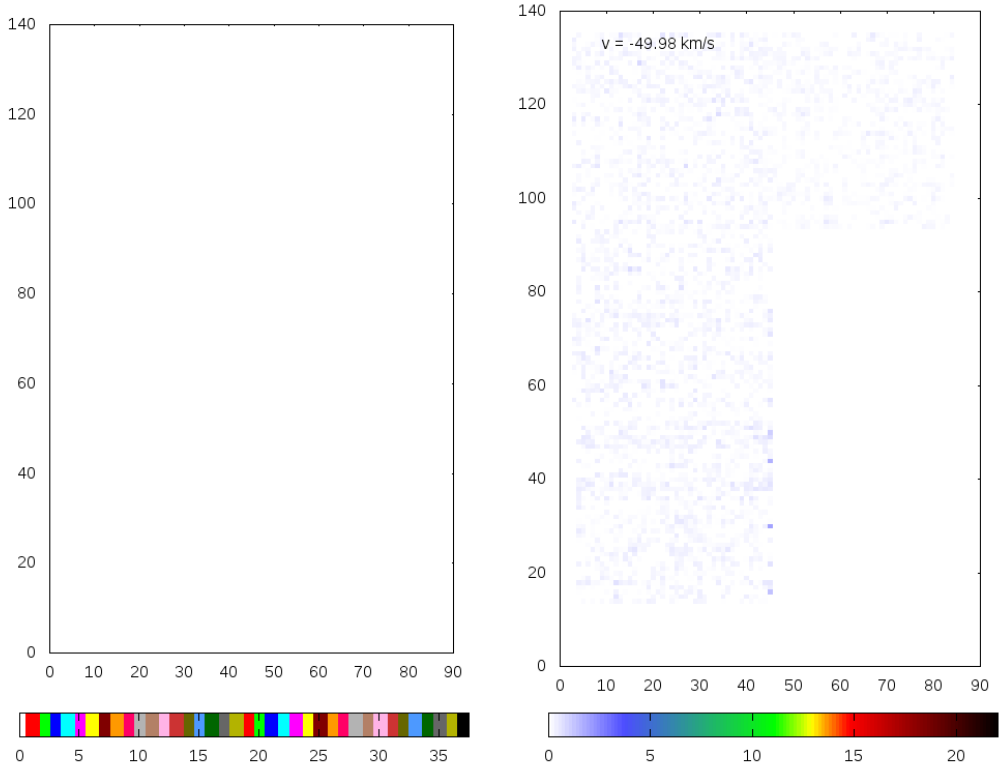

Mass spectrum and separation of clumps

- 44 clumps identified (after deleting clumps touching borders)
- clump mass function has slope ~ -1.7 (similar to Kramer et al. 1998) and peak at $m_{\rm peak} \sim 10$ M$_\odot$ (resolution limit ~ 0.5 M$_\odot$)
- separation of clumps: minimum spanning tree, $d_{\rm av} \sim 1.4$ pc

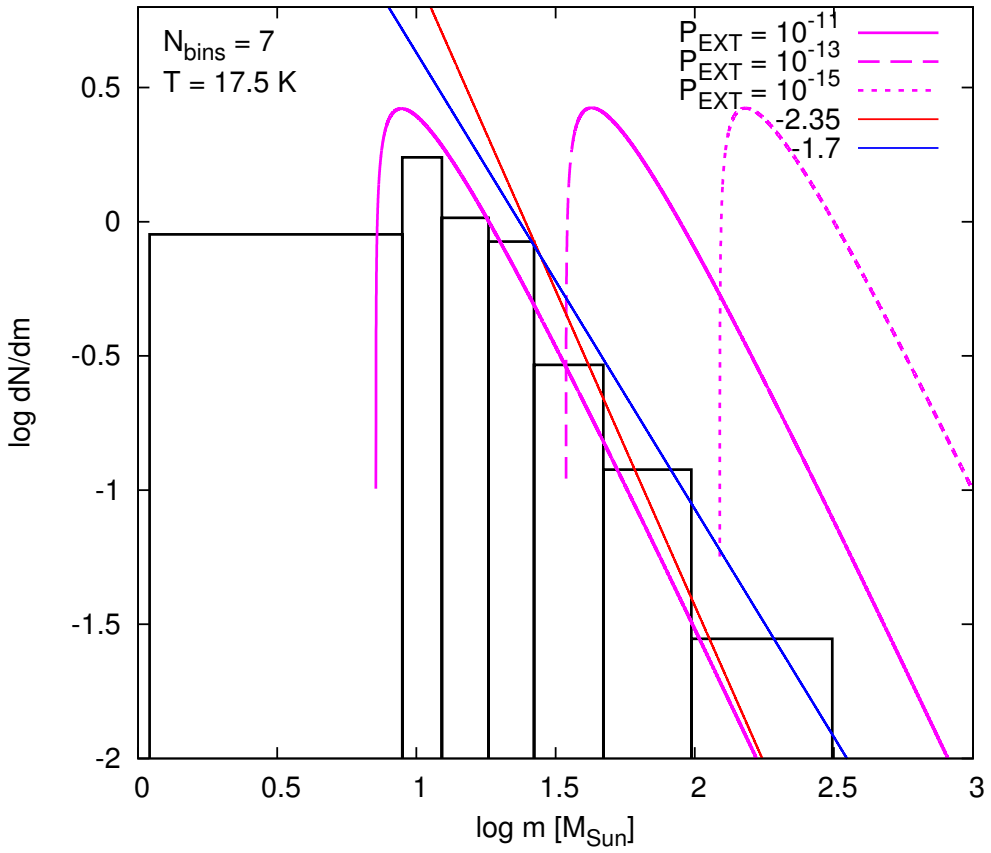

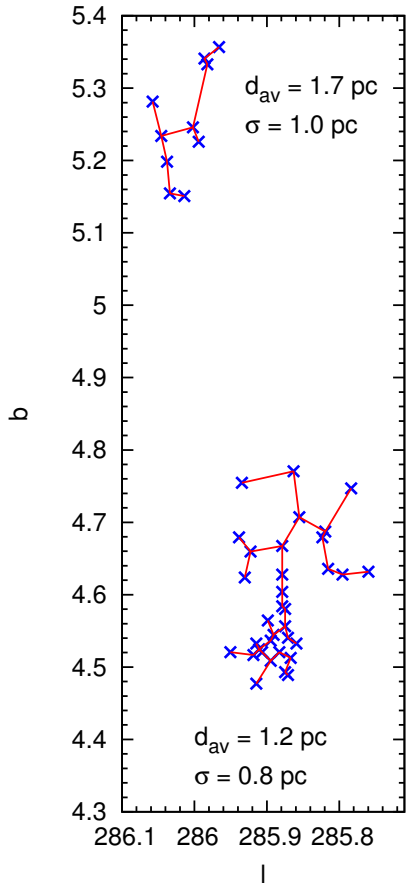

PAGI vs. observations

- PAGI: $\omega(l, \Sigma, P_{\rm EXT}, T_{\rm shell})$
- $m_{\rm peak} = 10$ M$_\odot$ and $d_{\rm av} = 1.4$ pc cross

  $\Rightarrow$ clump masses and separations consistent with PAGI!
- cross at $P_{\rm EXT} = 3 \times 10^{-12}$ dyne cm^{-2} and $\Sigma = 1.5 \times 10^{-3}$ g cm^{-2}

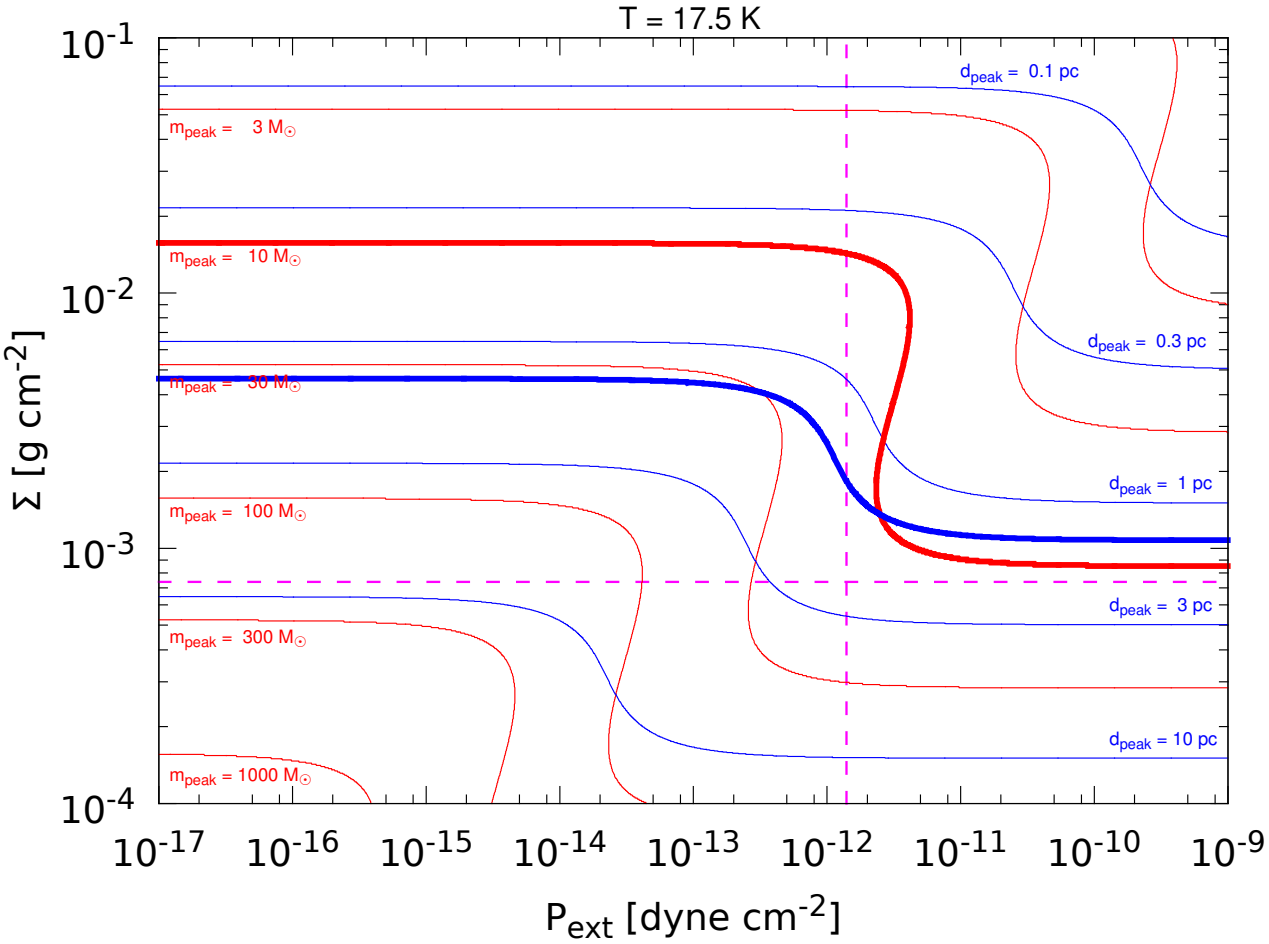

Discussion

- PAGI gives systematically larger range of unstable wavelengths than simulations (?approximation of the UOS evolution by constant acceleration)
- ω only amplifies initial spectrum (given by the turbulence, . . .)
- we assume shell confined by thermal pressure from both sides, but instability can be different if the ram pressure confines the shell from outside (accreting shell)
- Vishniac and RT instabilities may have an impact
- observations show that fragments in Cloud 16 are consistent with PAGI, however, other formation mechanisms are not ruled out
- future APEX observations of Cloud 74 and ALMA observations of both regions will provide more constrains on the theory

Conclusions

- excellent agreement between AMR and SPH, but disagreement with the thin shell approximation
- new instability (PAGI) and dispersion relation (fragment growth rate) for the thick shell embedded in the medium with non-zero pressure
- the PAGI dispersion relation depends on the external pressure, predicts range of unstable wavenumbers different than the one given by the thin shell approximation by factor of 0.6 and 2.2 for $P_{\rm ext} = 0$ and ∞, respectively
- the PAGI dispersion relation approaches to the thin shell one for $P_{\rm EXT}$ for which the shell thickness locally does not depend on Σ
- CO observations of Cloud 16 in Carina Flare supershell show that clumps have masses and separations consistent with PAGI
- observationally determined $P_{\rm EXT} \sim 3 \times 10^{-12}$ dyne cm^{-2} and $\Sigma \sim 1.5 \times 10^{-3}$ g cm^{-2} are close to expected values

References

Dale, J. E., Wünsch, R., Whitworth, A., Palouš, J., 2009, MNRAS, 398, 1537

Wünsch, R., Dale, J. E., Palouš, J., Whitworth, A., 2010, MNRAS, 407, 1963

Dale, J. E., Wünsch, R., Smith, R. J., Whitworth, A., Palouš, J., 2011, MNRAS, 411, 2230

Wünsch, R., Jáchym, P., Sidorin, V., Ehlerová, S., Palouš, J., Dale, J. E., Dawson, J. R., Fukui, Y., 2011, A&A, submitted

Boyd & Whitworth, 2005, A&A, 430, 1059
Churchwell, E., etal, 2006, ApJ, 649, 759
Deharveng, L., Lefloch, B.; Zavagno, A.; Caplan, J.; Whitworth, A. P.; Nadeau, D.; Martín, S.2003, A&A, 408, L25
Ehlerová, S., Palouš, J., 2005, A&A, 437, 101
Elmegreen, B. G., Lada, C. J., 1977, ApJ, 214, 725
Elmegreen, B. E., 1994, ApJ, 427, 384
Garcia-Segura, G., Franco, J., 1996, ApJ, 496, 171
Klessen, R., Burkert, A., 2000, ApJS, 128, 287
Kramer, C., Stutzki, J., Rohrig, R., Corneliussen, U., 1998, A&A, 329, 249
Parker, E. N., 1966, ApJ, 145, 811
Sidorin, V. 2008, Master thesis, Charles University
Smith, R. J., Clark, P. C., Bonnell, I. A., 2009, MNRAS, 396, 830
Vishniac, E. T., 1983, ApJ, 274, 152
Wardle, M. 1990, MNRAS, 246, 98